Table 2. ECG, Optical Repolarization, and Depolarization Parameters Just Before Polymorphic VT or VF in the Brugada-ECG Condition

	PVT (n = 12)	VF (n = 5)	p Value
VT/VF CL (ms)	325 ± 33	190 ± 23	<0.001
QRS duration (ms)	74 ± 18	102 ± 23	0.009
J-point (mV)	0.48 ± 0.31	0.43 ± 0.15	NS
Epi max-min APD_{50} (ms)	394 ± 79	344 ± 88	NS
Epi GR_{max} (ms/mm)	169 ± 55	157 ± 22	NS
Sti-Epi interval (ms)	43 ± 10	60 ± 16	0.03
Delta-Epi interval (ms)	13 ± 3	41 ± 16	0.001

Values are mean ± SD.
CL = averaged tachycardia cycle length; PVT = polymorphic ventricular tachycardia; VF = ventricular fibrillation; VT = ventricular tachycardia; other abbreviations as in Table 1.

grammed electrophysiologic stimulation (3,6,14,30), although it is still unclear how VF re-entry is maintained in the Brugada syndrome. In this study, most of the polymorphic VT was single or figure-of-eight type re-entry with no wave-break and terminated within a few seconds (Fig. 6C). In contrast, wave-break in VF group occurred during the first re-entrant wave and took place at sites of the delayed epicardial conduction (Fig. 7B). Wu et al. (31) demonstrated that Ca^{2+} and fast Na^{+} current inhibition turned fast VF into slow VF by flattering APD restitution and increasing conduction time. In this Brugada model, however, VF was characterized as the shorter cycle length and multiple wandering wavelets (Fig. 7C) in spite of the slower conduction (Fig. 8), because APD restitution was not flat but rather an "inverse" pattern (Fig. 9), thus increasing dispersion of repolarization during tachycardia. Krishnan and Antzelevitch (25) had demonstrated the incremental arrhythmogenesis of Na^{+} channel dysfunction in the RV epicardium during tachycardia. Flecainide also rate-dependently slowed down the conduction velocity. Thus, fast Na^{+} current inhibition strongly enhances both heterogeneity of repolarization and conduction slowing during tachycardia in the Brugada-ECG model, which can easily break up the spiral re-entry, thus degenerating polymorphic VT into VF with multiple wavelets.

Clinical implication. Previous clinical study suggested that induction of VF by programmed ventricular stimulation depended on the severity of depolarization abnormalities such as a longer QRS duration or His-ventricular interval but did not predict the recurrence of cardiac events in symptomatic Brugada syndrome (14,15). Moreover, depolarization and repolarization abnormalities in this syndrome are now considered to be closely correlated (16,29,32,33), supporting our data that both repolarization and depolar-

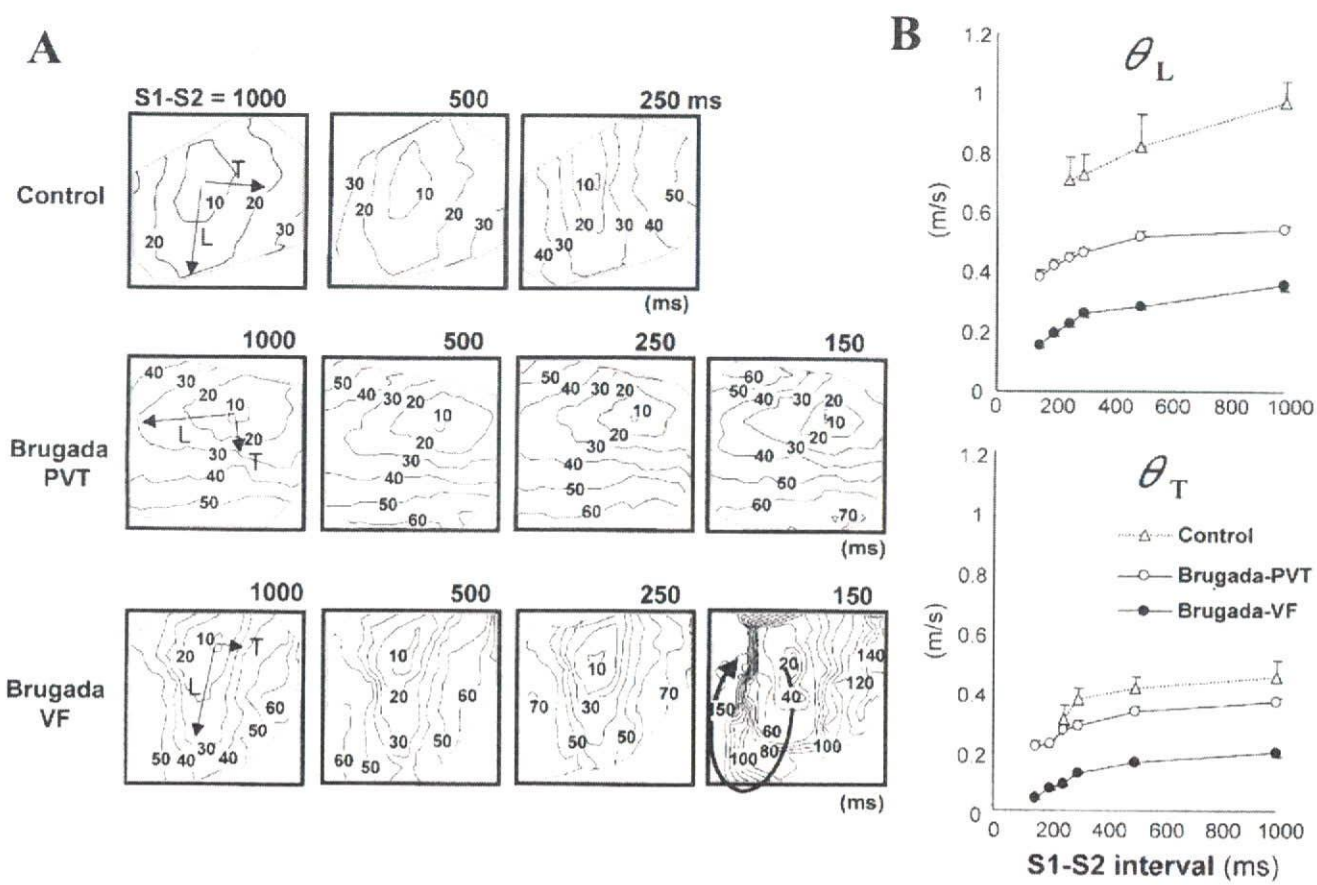

Figure 8. Representative epicardial depolarization maps paced from the epicardium by S1-S2 method in the control and ST-segment elevation (Brugada-ECG) condition with polymorphic ventricular tachycardia (PVT) or ventricular fibrillation (VF) **(A)**, and longitudinal (L) and transverse (T) conduction velocity (θ) restitution curves in each condition **(B)**. Values are mean ± SEM.

JACC Vol. 47, No. 10, 2006
May 16, 2006:2074–85

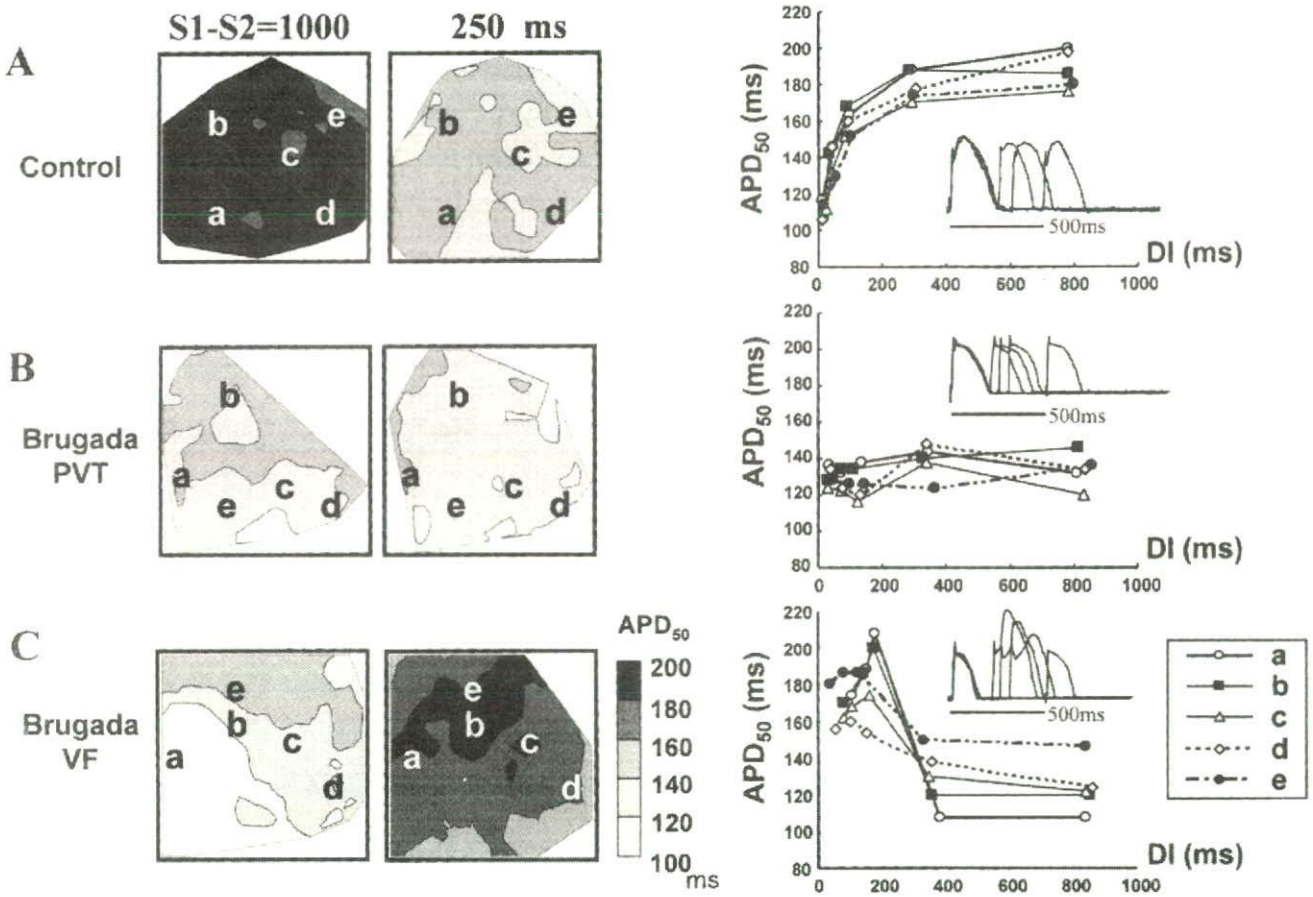

Figure 9. Representative epicardial repolarization maps paced from the epicardium by S1-S2 method and plot of the restitution of action potential duration at each site **(a to e)** and superimposed optical action potentials at site b in control condition **(A)**, and the Brugada-ECG condition with polymorphic ventricular tachycardia (PVT) **(B)** or ventricular fibrillation (VF) **(C)**. APD_{50} = action potential duration at 50% repolarization; DI = diastolic interval.

ization abnormalities were important in the development of VF. Our results, for the first time, revealed how repolarization and depolarization abnormalities interact in developing a trigger of premature ventricular complexes and in maintaining VF in the Brugada-ECG condition. A steep repolarization gradient in the epicardium introduced P2R-extrasystoles and subsequent non-sustained polymorphic VT, and further increased depolarization and repolarization abnormalities maintained VF, thus increasing risk of sudden cardiac death.

Study limitations. First, we mapped the epicardial or endocardial surface separately in each condition. Therefore, the two-dimensional mapping technique used in this study provides only limited insights into the number of spiral waves and these re-entrant patterns and could not directly evaluate the relationship between the transmural gradient of repolarization and arrhythmogenesis in the Brugada-ECG condition. A second limitation is the size of wedge preparation. It is unclear whether a polymorphic VT or VF in the wedges can result in those with larger hearts. Third, we pharmacologically created, similarly to the methods of previous studies, the Brugada-phenotype, which could not be a complete surrogate for the Brugada syndrome. Finally, with optical mapping, there is a major concern about motion artifacts that can greatly distort the AP recorded, but our ratio-metric methods can reduce motion artifacts without using an uncoupler.

Reprint requests and correspondence: Dr. Wataru Shimizu, Division of Cardiology, Department of Internal Medicine, National Cardiovascular Center, 5-7-1 Fujishiro-dai, Suita, Osaka, 565-8565 Japan. E-mail: wshimizu@hsp.ncvc.go.jp.

REFERENCES

1. Brugada P, Brugada J. Right bundle branch block, persistent ST-segment elevation and sudden cardiac death: a distinct clinical and electrocardiographic syndrome. A multicenter report. J Am Coll Cardiol 1992;20:1391–6.
2. Wilde AA, Antzelevitch C, Borggrefe M, et al. Proposed diagnostic criteria for the Brugada syndrome: consensus report. Circulation 2002; 106:2514–9.
3. Brugada J, Brugada R, Antzelevitch C, Towbin J, Nademanee K, Brugada P. Long-term follow-up of individuals with the electrocardiographic pattern of right bundle-branch block and ST-segment elevation in precordial leads V1 to V3. Circulation 2002;105:73–8.
4. Antzelevitch C, Brugada P, Borggrefe M, et al. Brugada syndrome: report of the second consensus conference: endorsed by the Heart Rhythm Society and the European Heart Rhythm Association. Circulation 2005;111:659–70.
5. Brugada J, Brugada R, Brugada P. Determinants of sudden cardiac death in individuals with the electrocardiographic pattern of Brugada

syndrome and no previous cardiac arrest. Circulation 2003;108: 3092–6.
6. Priori SG, Napolitano C, Gasparini M, et al. Natural history of Brugada syndrome: insights for risk stratification and management. Circulation 2002;105:1342–7.
7. Antzelevitch C, Brugada P, Brugada J, Brugada R, Towbin JA, Nademanee K. Brugada syndrome: 1992–2002: a historical perspective. J Am Coll Cardiol 2003;41:1665–71.
8. Yan GX, Antzelevitch C. Cellular basis for the Brugada syndrome and other mechanisms of arrhythmogenesis associated with ST-segment elevation. Circulation 1999;100:1660–6.
9. Di Diego JM, Cordeiro JM, Goodrow RJ, et al. Ionic and cellular basis for the predominance of the Brugada syndrome phenotype in males. Circulation 2002;106:2004–11.
10. Fish JM, Antzelevitch C. Role of sodium and calcium channel block in unmasking the Brugada syndrome. Heart Rhythm 2004;1:210–7.
11. Kurita T, Shimizu W, Inagaki M, et al. The electrophysiologic mechanism of ST-segment elevation in Brugada syndrome. J Am Coll Cardiol 2002;40:330–4.
12. Lukas A, Antzelevitch C. Phase 2 re-entry as a mechanism of initiation of circus movement re-entry in canine epicardium exposed to simulated ischemia. Cardiovasc Res 1996;32:593–603.
13. Nademanee K, Veerakul G, Nimmannit S, et al. Arrhythmogenic marker for the sudden unexplained death syndrome in Thai men. Circulation 1997;96:2595–600.
14. Kanda M, Shimizu W, Matsuo K, et al. Electrophysiologic characteristics and implications of induced ventricular fibrillation in symptomatic patients with Brugada syndrome. J Am Coll Cardiol 2002;39: 1799–805.
15. Ikeda T, Sakurada H, Sakabe K, et al. Assessment of noninvasive markers in identifying patients at risk in the Brugada syndrome: insight into risk stratification. J Am Coll Cardiol 2001;37:1628–34.
16. Nagase S, Kusano KF, Morita H, et al. Epicardial electrogram of the right ventricular outflow tract in patients with the Brugada syndrome: using the epicardial lead. J Am Coll Cardiol 2002;39:1992–5.
17. Smits JP, Eckardt L, Probst V, et al. Genotype-phenotype relationship in Brugada syndrome: electrocardiographic features differentiate SCN5A-related patients from non-SCN5A-related patients. J Am Coll Cardiol 2002;40:350–6.
18. Akar FG, Spragg DD, Tunin RS, Kass DA, Tomaselli GF. Mechanisms underlying conduction slowing and arrhythmogenesis in nonischemic dilated cardiomyopathy. Circ Res 2004;95:717–25.
19. Kimura M, Kobayashi T, Owada S, et al. Mechanism of ST elevation and ventricular arrhythmias in an experimental Brugada syndrome model. Circulation 2004;109:125–31.
20. Gray RA, Pertsov AM, Jalife J. Spatial and temporal organization during cardiac fibrillation. Nature 1998;392:75–8.
21. Liu YB, Peter A, Lamp ST, Weiss JN, Chen PS, Lin SF. Spatiotemporal correlation between phase singularities and wavebreaks during ventricular fibrillation. J Cardiovasc Electrophysiol 2003;14:1103–9.
22. Pitzalis MV, Anaclerio M, Iacoviello M, et al. QT-interval prolongation in right precordial leads: an additional electrocardiographic hallmark of Brugada syndrome. J Am Coll Cardiol 2003;42:1632–7.
23. Kakishita M, Kurita T, Matsuo K, et al. Mode of onset of ventricular fibrillation in patients with Brugada syndrome detected by implantable cardioverter defibrillator therapy. J Am Coll Cardiol 2000;36: 1646–53.
24. Morita H, Fukushima-Kusano K, Nagase S, et al. Site-specific arrhythmogenesis in patients with Brugada syndrome. J Cardiovasc Electrophysiol 2003;14:373–9.
25. Krishnan SC, Antzelevitch C. Flecainide-induced arrhythmia in canine ventricular epicardium. Phase 2 re-entry? Circulation 1993;87: 562–72.
26. Miyoshi S, Mitamura H, Fujikura K, et al. A mathematical model of phase 2 re-entry: role of L-type Ca current. Am J Physiol Heart Circ Physiol 2003;284:H1285–94.
27. Chen Q, Kirsch GE, Zhang D, et al. Genetic basis and molecular mechanism for idiopathic ventricular fibrillation. Nature 1998;392: 293–6.
28. Brugada R, Brugada J, Antzelevitch C, et al. Sodium channel blockers identify risk for sudden death in patients with ST-segment elevation and right bundle branch block but structurally normal hearts. Circulation 2000;101:510–5.
29. Shimizu W, Antzelevitch C, Suyama K, et al. Effect of sodium channel blockers on ST segment, QRS duration, and corrected QT interval in patients with Brugada syndrome. J Cardiovasc Electrophysiol 2000; 11:1320–9.
30. Gasparini M, Priori SG, Mantica M, et al. Programmed electrical stimulation in Brugada syndrome: how reproducible are the results? J Cardiovasc Electrophysiol 2002;13:880–7.
31. Wu TJ, Lin SF, Weiss JN, Ting CT, Chen PS. Two types of ventricular fibrillation in isolated rabbit hearts: importance of excitability and action potential duration restitution. Circulation 2002;106: 1859–66.
32. Hisamatsu K, Kusano KF, Morita H, et al. Relationships between depolarization abnormality and repolarization abnormality in patients with Brugada syndrome. J Cardiovasc Electrophysiol 2004;15:870–6.
33. Tukkie R, Sogaard P, Vleugels J, de Groot IK, Wilde AA, Tan HL. Delay in right ventricular activation contributes to Brugada syndrome. Circulation 2004;109:1272–7.

APPENDIX

For accompanying videos to Figures 5, 6, and 7, please see the online version of this article.

Circ J 2007; **Suppl A:** A-32–A-39

Mechanism and New Findings in Brugada Syndrome

Wataru Shimizu, MD; Takeshi Aiba, MD; Shiro Kamakura, MD

Brugada syndrome is a clinical entity characterized by coved type ST-segment elevation in the right precordial electrocardiographic leads (V_{1-3}) and an episode of ventricular fibrillation in the absence of structural heart disease. Although a number of clinical and experimental reports have elucidated the electrocardiographic, electrophysiologic, cellular, and molecular aspects, several problems remain unsolved. Recently developed high-resolution optical mapping techniques in arterially-perfused wedge preparations enable recording of transmembrane action potentials from 256 sites simultaneously at the epicardial surface, thus providing further advances in the understanding of the cellular mechanism of the specific ST-segment elevation and subsequent ventricular arrhythmias. In this review article, new findings relating to several unresolved problems such as gender difference (male predominance) and ethnic difference (higher incidence in Asian population) are also presented. (*Circ J* 2007; **Suppl A:** A-32–A-39)

Key Words: Brugada syndrome; Ethnicity; Gender; Genetics; Mutation; Polymorphism; ST-segment; Ventricular fibrillation

Brugada syndrome (BS) is characterized by coved-type ST-segment elevation in the right precordial electrocardiography (ECG) leads (V_{1-3}) and an episode of ventricular fibrillation (VF) in the absence of acute ischemia, electrolyte abnormalities or structural heart disease[1–8] A type-1 ST-segment elevation, which is defined as a coved ST-segment elevation of ≥0.2 mV at the J point with or without a terminal negative T wave, is required to diagnose BS, regardless of the absence or presence of sodium-channel blockers (Figs 1A,B)[7] A type-1 ST-segment elevation recorded only in the higher V_{1-2} leads (ie, 3rd and 2nd intercostal spaces) has been suggested to show similar prognostic value for subsequent cardiac events as that recorded in the standard V_{1-2} leads (Fig 1C)[7,9,10] A type-2 saddle-back ST-segment elevation alone is not diagnostic for BS (Fig 1B). The prevalence of this syndrome is estimated to be 5 per 10,000 inhabitants, and is one of the important causes of sudden cardiac death of middle-aged males in Asian countries particularly[11,12] BS usually manifests during adulthood, with a mean age of sudden death of 41±15 years, and child cases are rare[7] A family history of unexplained sudden death is present in approximately 20–40% of the population in Western countries, and less (15–20%) in Japan[4,7,13,14] A significant male predominance in BS has long been reported, and more than 80% of patients in Western countries and more than 90% of patients in Asian countries affected with BS are men[15] Since Brugada and Brugada described 8 patients with a history of aborted sudden cardiac death caused by VF as a distinct clinical entity in 1992[1] a number of clinical and experimental reports from around the world have demonstrated the clinical, electrocardiographic, electrophysiologic, cellular, ionic, genetic and molecular features of BS[2–14] However, several problems remain unsolved, such as genetic heterogeneity, late onset of first cardiac events, and gender and ethnic differences[8] In this review article, we present our recent data relating to the cellular and molecular mechanism of BS, the late onset of its clinical manifestation, male predominance, and higher incidence in Asian populations.

(Received January 25, 2007; revised manuscript received February 7, 2007; accepted February 8, 2007)

Division of Cardiology, Department of Internal Medicine, National Cardiovascular Center, Suita, Japan
Mailing address: Wataru Shimizu, MD, Division of Cardiology, Department of Internal Medicine, National Cardiovascular Center, 5-7-1 Fujishiro-dai, Suita 565-8565 Japan. E-mail: wshimizu@hsp.ncvc.go.jp

Genetic and Molecular Aspects

Advances in molecular genetics in the past decade have established a link between several inherited cardiac arrhythmias, including BS and long QT syndrome, and mutations in genes encoding ion channels, membrane components or receptors[16] In 1998, the first mutation linked to BS was identified by Chen et al in *SCN5A*[17] the gene encoding the α subunit of the sodium channel. Thereafter, a large family of BS was reported to link to a second locus on chromosome 3, which is close to but different from the *SCN5A* locus;[18] however, specific gene or genes other than *SCN5A* have not yet been identified on chromosome 3. *SCN5A* mutations are reported to account for 18–30% of clinically diagnosed BS patients at present[7] Antzelevitch et al have recently reported that 3 probands associated with a BS-like ST-segment elevation and a short QT interval were linked to mutations in *CACNA1C* (A39V and G490R) or *CACNB2* (S481L), the gene encoding the α1 or β2b subunit of the L-type calcium channel, respectively[19] Their genetic and heterologous expression studies revealed loss of function of the L-type calcium channel current (I_{Ca-L}). However, approximately two-thirds of BS patients have not been yet genotyped, suggesting the presence of genetic heterogeneity[8] Other candidate genes for the Brugada phenotype include those encoding the transient outward current (I_{to}) and the delayed rectifier potassium current (I_K), or those coding the adrenergic receptors, cholinergic receptors, ion-channel-interacting protein, promoters, transcriptional factors, neurotransmitters, or transporters[7,8]

Among the approximately 100 mutations in *SCN5A* linked to BS, some of them have been studied in expression systems, and have been shown to result in loss of function of the sodium channel current (I_{Na}) by several mechanisms[20]

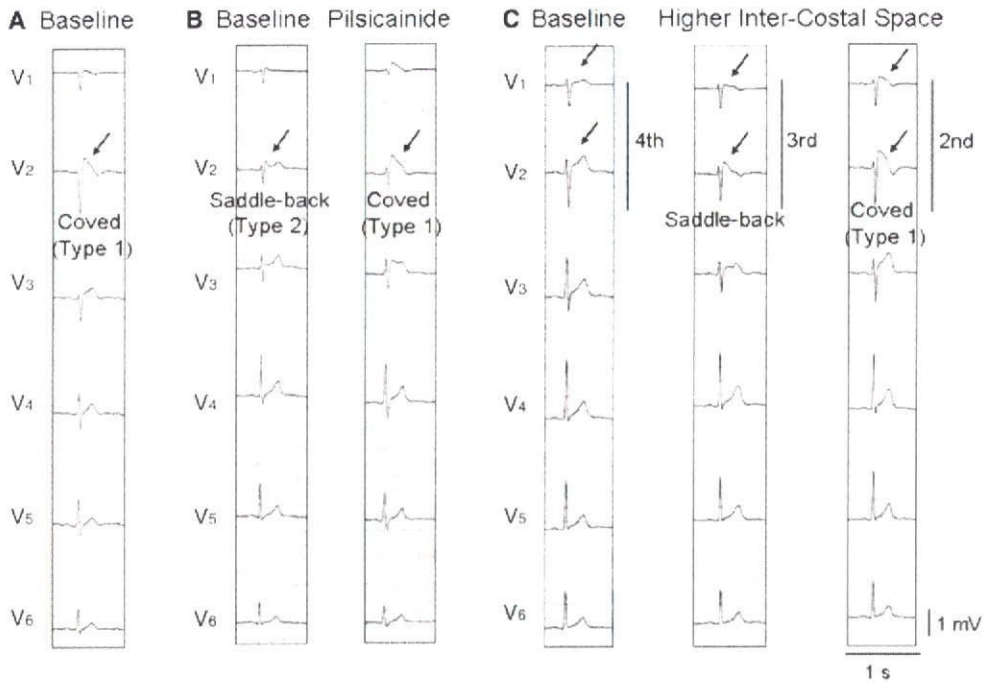

Fig 1. (A) Spontaneous type 1 coved type ST-segment elevation (arrow). (B) Unmasking of ST-segment elevation by a class IC sodium-channel blocker, pilsicainide. Under baseline conditions, type 2 saddle-back type ST-segment elevation is recorded in lead V_2 (Left, arrow). Pilsicainide injection (30 mg) unmasks the type 1 coved type ST-segment elevation in lead V_2 (Right, arrow). (C) Unmasking of the type 1 electrocardiogram (ECG) by recording the right precordial (V_{1-3}) leads at the 3rd and 2nd intercostal spaces. No significant ST-segment elevation is observed in leads V_1 and V_2 of the standard 12-lead ECG (4th intercostal space) (Left, arrow), whereas saddle-back type (Middle, arrow) and type 1 coved type (Right, arrow) ST-segment elevation are unmasked in leads V_1 and V_2 recorded from the 3rd and 2nd intercostal spaces, respectively.

These functional effects include: (1) lack of expression of the sodium channel; (2) a shift in the voltage-dependence and time-dependence of I_{Na} activation, inactivation or reactivation; (3) entry of the sodium channel into an intermediate state of inactivation from which it recovers more slowly; (4) accelerated inactivation of the sodium channel; and (5) a trafficking defect. Some common *SCN5A* polymorphisms are reported to modulate the functional consequences of primary *SCN5A* mutations. Baroudi et al first suggested that the interaction of *SCN5A* polymorphisms and *SCN5A* mutations may affect the consequence of the functional effects. They reported that a common polymorphism (R1232W) of *SCN5A* affected protein trafficking when it was co-expressed with a T1620M mutation, although the T1620M mutation alone produced only gating abnormalities in the I_{Na}.[21] On the other hand, another common polymorphism (H558R) of *SCN5A* was reported by Ye et al to rescue normal trafficking and normal I_{Na} for the M1766L mutant protein.[22] These effects of common *SCN5A* polymorphisms on modifying the functional consequence of *SCN5A* mutations may make the clinical phenotype more complex.

Cellular Mechanism of Brugada Phenotype

The I_{to}-mediated phase 1 notch of the action potential (AP) has been reported to be larger in the epicardium than in the endocardium in many species, including humans.[23] Because the maintenance of the AP dome is determined by the fine balance of currents active at the end of phase 1 of the AP (principally I_{to} and $I_{Ca\text{-}L}$), any interventions that cause a net outward shift in the current active at the end of phase 1 can increase the magnitude of the AP notch, leading to loss of the AP dome (all-or-none repolarization) in the epicardium, but not in the endocardium, contributing to a significant voltage gradient across the ventricular wall during ventricular activation.[23] The heterogeneous loss of the AP dome in the epicardium has been shown to produce premature beats via a mechanism of phase 2 reentry in experimental studies using isolated sheets of canine right ventricle.[24] Therefore, these mechanism of all-or-none repolarization in the epicardial cells and phase 2 reentry-induced premature beat between the adjacent epicardial cells were expected to be responsible for the clinical phenotype in BS.

In the late 1990s, Antzelevitch's group developed an experimental model of BS using arterially perfused canine right ventricular (RV) wedge preparations, in which transmembrane APs and pseudo-ECGs were simultaneously recorded. These experimental studies have provided significant insights of the cellular mechanism of the Brugada phenotype, ST-segment elevation and subsequent VF.[25,26] The I_{to}-mediated AP notch and the loss of the AP dome in the epicardial cells, but not in the endocardial cells, of the right ventricle gives rise to a transmural voltage gradient, producing ST-segment elevation in the ECG in the wedge preparations. Fig 2 shows transmembrane APs simultaneously recorded from 2 epicardial (Epi) and 1 endocardial sites, together with a transmural ECG in a Brugada model using the RV wedge preparation. Under control conditions, a small J wave coincides with the small notch observed in the epicardial cells, but not in the endocardial cells (Fig 2A). Combined administration of terfenadine ($I_{Ca\text{-}L}$ block) and pilsicainide (I_{Na} block) produces a loss of the AP dome in

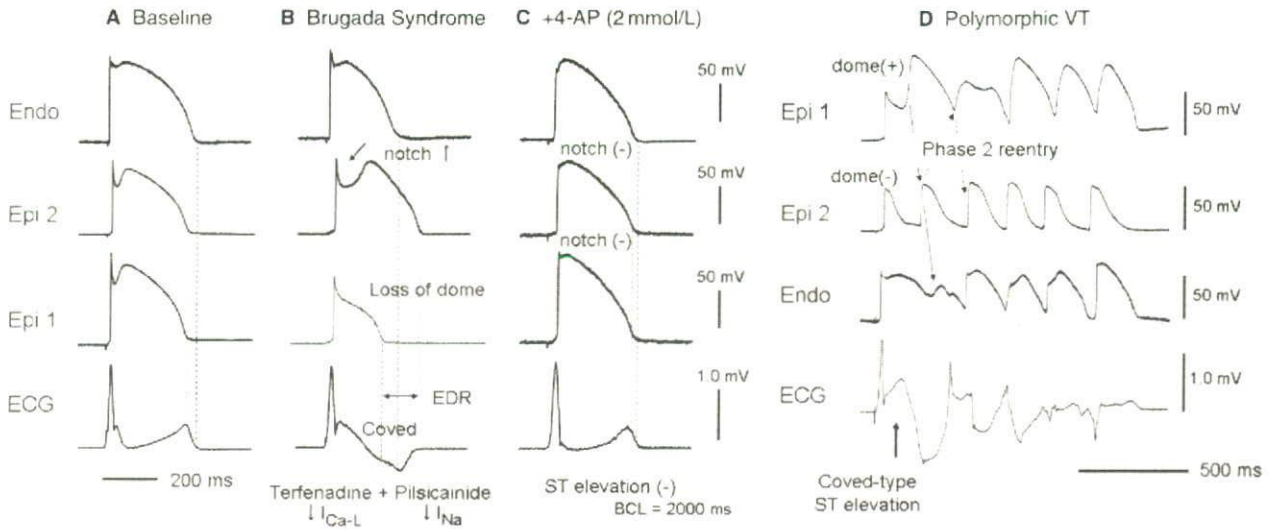

Fig 2. Type 1 coved type ST-segment elevation and non-sustained polymorphic ventricular tachycardia (VT) via phase 2 reentry induced in a Brugada model using an arterially perfused canine right ventricular wedge preparation. Shown are transmembrane action potentials (APs) simultaneously recorded from 2 epicardial sites (Epi 1 and Epi 2) and 1 endocardial site (Endo) together with a transmural ECG (basic cycle length (BCL) = 2,000 ms). (A) Under baseline conditions, phase 1 AP notch in Epi, but not in Endo, is associated with a J wave in the ECG. (B) Combined administration of terfenadine (5 μmol/L) and pilsicainide (5 μmol/L) produces a loss of AP dome in Epi 1, but not in Epi 2, resulting in a marked epicardial dispersion of repolarization (EDR), and a coved-type ST segment elevation and a negative T wave in the ECG. (C) 4-aminopyridine (4-AP), a selective blocker of the transient outward current (I_{to}) (2 mmol/L), restores the AP dome, decreases the phase 1 AP notch, and normalizes the ST-segment elevation. (D) In the setting of heterogeneous loss of the AP dome (coexistence of loss of dome regions and restored dome regions) in the epicardium and a remarkable coved type ST-segment elevation in the ECG with combined administration with terfenadine and pilsicainide, electrotonic propagation from the site where the dome is restored (Epi 1) to the site where it is lost (Epi 2) results in development of a premature beat induced by phase 2 reentry, triggering spontaneous polymorphic VT (Modified from *Nat Clin Pract Cardiovasc Med* 2005; **2**: 408–414 with permission).

Epi 1, but not in Epi 2, resulting in a marked epicardial dispersion of repolarization (EDR), and a coved-type ST segment elevation and negative T wave in the ECG (Fig 2B). A selective I_{to} blocker, 4-aminopyridine, restores the AP dome, decreases the phase 1 AP notch, and normalizes the ST-segment elevation (Fig 2C). Fig 2D shows non-sustained polymorphic ventricular tachycardia (VT) via phase 2 reentry induced in a Brugada model using the wedge preparation. In the setting of remarkable coved type ST-segment elevation with combined administration of terfenadine and pilsicainide, heterogeneous loss of the AP dome (coexistence of loss of dome regions and restored dome regions) in the epicardium creates a marked EDR, giving rise to premature beats caused by phase 2 reentry, which precipitates non-sustained polymorphic VT.

Optical Mapping Study

The AP data in the Brugada model using arterially perfused canine RV wedge preparations strongly supported the hypothesis that episodes of VF in BS are triggered by premature beats between the adjacent epicardial cells via the mechanism of phase 2 reentry. However, the precise mechanism of the initial premature beats and the maintenance of non-sustained polymorphic VT or VF remain unsolved, because the number of AP recording sites available for floating microelectrodes is small in the wedge preparations. To overcome this limitation, we recently developed high-resolution (256×256) optical mapping techniques that allowed us to record transmembrane APs from 256 sites simultaneously at the epicardial or endocardial surface of the wedge preparations (Figs 3–5)[8,27] Fig 3 shows the mechanism of phase 2 reentry-induced premature beats (P2R-extrasystoles) under Brugada-ECG conditions. A steep repolarization gradient between the loss of dome region and the restored dome region in the epicardium, but not in the endocardium, develops the initial P2R-extrasystole. We then recorded spontaneous episodes of P2R-extrasystoles and subsequent non-sustained polymorphic VT or VF under these conditions, and analyzed the epicardial AP duration (APD) and conduction velocity (Figs 4,5). Once again, most of the P2R-extrasystoles originated from the area showing the steepest (maximum) gradient of repolarization (GR_{max}) between the loss of dome site and the restored dome site in the epicardium (Figs 4C,5C, arrows), leading to non-sustained polymorphic VT or VF. These data also indicate that a steep repolarization gradient between the loss of dome region and the restored dome region in the epicardium is essential to produce the P2R-extrasystoles that precipitate polymorphic VT or VF. On the other hand, the epicardial GR_{max} does not differ between episodes of polymorphic VT and those of VF. Figs 4D,E and 5D,E show the mechanism underlying the difference between polymorphic VT and VF. Just before inducing the episodes of polymorphic VT or VF, the epicardial depolarization map paced from the endocardium at the basic cycle length of 2,000 ms shows a remarkable conduction delay in the episode of VF (Fig 5D) compared with that of polymorphic VT (Fig 4D). The conduction parameters, such as QRS duration and interval between the stimulus and the earliest epicardial activation, are significantly longer in the episodes of VF than in those of polymorphic VT. Figs 4A,B

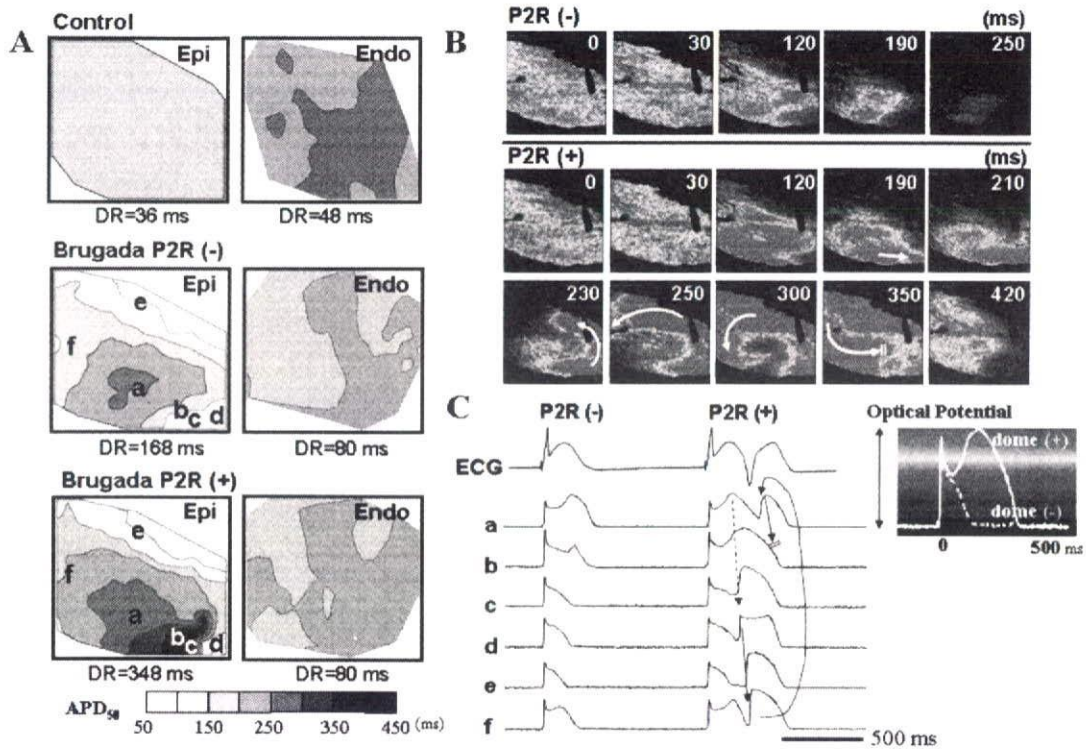

Fig 3. Mechanism of the phase 2 reentry-induced premature beats (P2R-extrasystoles) under the condition of Brugada-ECG in a model using a wedge preparation combined with high-resolution (256×256) optical mapping techniques. (A) Representative action potential duration measured at 50% (APD_{50}) contour map on the right ventricular epicardium (Epi) and endocardium (Endo) in the control, in the ST-segment elevation (Brugada-ECG) without phase 2 reentrant extrasystoles (P2R (−)) and in the Brugada-ECG just before P2R extrasystoles (P2R (+)). (B) Snapshots of an optical isopotential movie on the Epi surface during P2R(−) and P2R(+) in the Brugada-ECG. (C) Optical action potentials (APs) at each site (a–f) on the Epi surface and transmural ECG. Under the Brugada-ECG, the AP morphology in Epi, but not Endo, changes to heterogeneous because of the combination of abbreviated (loss-of-dome; site d,e) and prolonged (restore-of-dome; site a,b) APs, resulting in increasing dispersion of repolarization (DR) in Epi (168 ms) rather than in Endo (80 ms). Further prolongation of the AP in the Epi area (site b) is closely adjacent to the loss-of-dome APs (site d), thus producing a repolarization mismatch within a small area (DR = 348 ms) and developing a P2R-extrasystole at the loss-of-dome site (site d). Thus, a steep repolarization gradient in Epi, but not in Endo, develops the initial P2R-extrasystole in the Brugada-ECG (Modified from *J Am Coll Cardiol* 2006; **47**: 2074–2085 with permission).

represents a phase map and the optical APs during the P2R-induced polymorphic VT, showing that reentry is initiated from the epicardial GR_{max} area and rotates mainly in the epicardium without wave-break. In contrast, Figs 5A,B represents these during P2R-induced VF, showing that the development of the initial P2R is similar to that of polymorphic VT, but that the first P2R-wave is broken up into multiple wavelets, resulting in degeneration of VT into VF. The phase singularity points during the first P2R-wave almost coincide with the sites of delayed conduction (Fig 5D). Wave-break during the first P2R-extrasystole produces multiple wavelets in the episodes of VF, whereas no wave-break or wave-break followed by wave collision and termination occurs in the episodes of polymorphic VT. Figs 4E and 5E are histograms of the epicardial APD measured at 50% (APD_{50}) during the first P2R-wave. There is a large variety of APD_{50} in the epicardium during the first P2R-wave in the episodes of VF, whereas only slight variety in the APD_{50} is observed in the episodes of polymorphic VT. These data suggest that both conduction delay and dispersion of repolarization play significant roles in the perpetuation of VF episodes.

Late Onset of Clinical Manifestation

Because BS is a primary electrical disease, and at least one-third of the patients have mutations in ion channel genes (*SCN5A*, *CACNA1C*, *CACNB2*), clinical manifestation during childhood would be expected. However, BS usually manifests in middle age, at 40–50 years of age[7] Frustaci et al recently reported a significant myocytes apotosis in both the right and left ventricular myocardium in a histological study of BS patients with *SCN5A* mutations, and suggested that abnormal function of the sodium channels may lead to a sufficient degree of cellular damage, attributing to the arrhythmic event.[28] We recently analyzed several ECG parameters recorded during long-term follow-up of BS patients with and without the *SCN5A* mutation.[29] In both patient groups, the depolarization parameters, including P wave, QRS, S wave duration and PQ interval, increased with age, especially in patients with the *SCN5A* mutation. Taken together with the experimental data,[27] the findings suggest that depolarization abnormalities (conduction slowing) are required for the maintenance of VF in BS, although the initiating premature beats are caused by a phase 2 reentry mechanism.

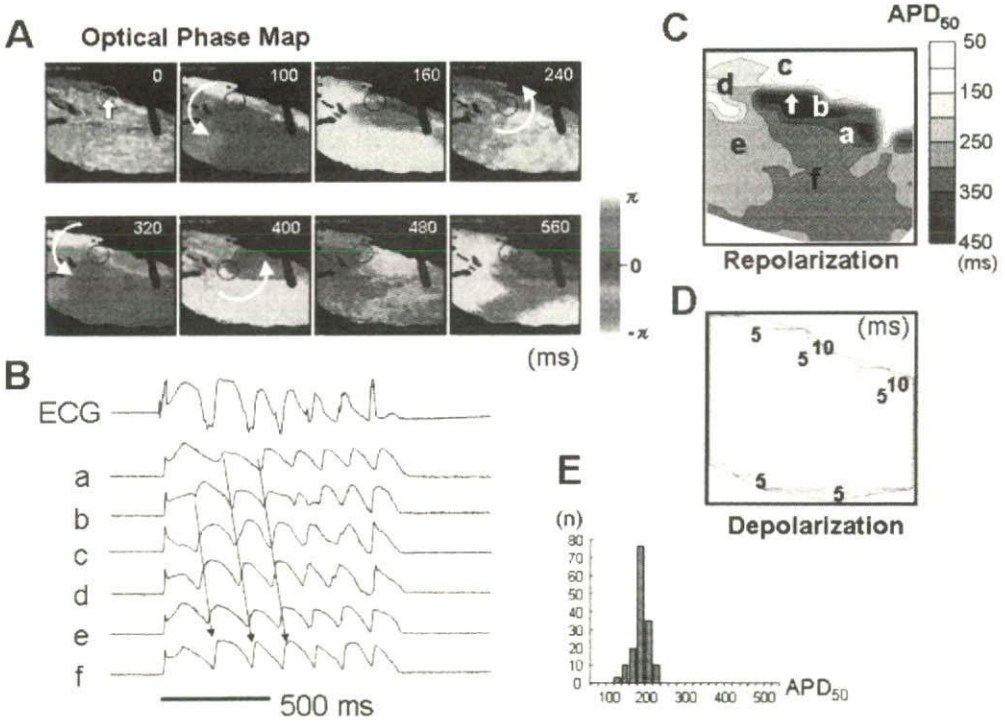

Fig 4. Mechanism underlying non-sustained polymorphic ventricular tachycardia (VT) in a Brugada model using a wedge preparation combined with high-resolution (256×256) optical mapping techniques. (A) Representative snapshots from a phase movie during polymorphic VT originating from epicardial (Epi) phase 2 reentry (P2R). (B) Optical action potentials at each site (a–f), together with a transmural ECG. (C, D) Repolarization and depolarization maps on the Epi surface in the condition of Brugada-ECG just before polymorphic VT. (E) Epi action potential duration at 50% repolarization (APD_{50}) histogram during the first P2R-wave. Reentry is initiated from the steepest (maximum) repolarization gradient site in Epi (arrow in A and C) and rotates mainly in Epi without wave-break. The Epi depolarization map paced from Endo shows no conduction delay (D). There is a little variety of APD in Epi during the first P2R-wave (E). Open circles mark phase singularity points (Modified from *J Am Coll Cardiol* 2006; **47:** 2074–2085 with permission).

Male Predominance

Because all mutations so far identified in *SCN5A* display an autosomal dominant mode of transmission in BS, males and females would be expected to inherit the defective gene equally. However, an apparent male predominance is observed in patients with BS.[15] Di Diego et al suggested the cellular basis for male predominance in BS while using arterially-perfused canine RV wedge preparations.[30] They reported that the I_{to}-mediated phase 1 AP notch in the RV epicardium was larger in male dogs than in female dogs was responsible for the male predominance in the Brugada phenotype. On the other hand, the male hormone, testosterone, has been reported to increase the outward potassium currents (the rapidly [I_{Kr}][31,32] and the slowly [I_{Ks}][33] activating component of I_K, and the inward rectifier potassium current [I_{K1}][32]) or decrease the inward currents ($I_{Ca\text{-}L}$).[33] Therefore, testosterone would be expected to accentuate the Brugada phenotype. Clinically, Matsuo et al report 2 cases of asymptomatic BS in which typical coved ST-segment elevation disappeared following orchiectomy as therapy for prostate cancer,[34] supporting the expectation for testosterone. Moreover, testosterone is also known to decrease visceral fat,[35] and patients with BS are thinner than the normal population.[36] On the basis of these clinical and experimental findings, we directly measured the testosterone level in male patients with BS and compared them with age-matched normal males.[37] The testosterone level was significantly higher and body mass index (BMI) significantly lower in the Brugada males than in the controls after adjusting for several confounding variables influencing testosterone level or BMI (eg, age, exercise, stress, smoking, and medication). Interestingly, testosterone level was inversely correlated with BMI in both Brugada and control males even after adjusting for confounding variables, suggesting that Brugada males have a higher testosterone level associated with lower visceral fat (Fig 6). Moreover, conditional logistic regression model analysis showed that both higher testosterone level and lower BMI independently increase the risk of BS. These data suggest that the male predominance in the Brugada phenotype is at least in part related to testosterone, which is present only in males.

Higher Incidence in Asian Population

The incidence of BS is higher in Asian countries, including Thailand and Japan, than in Western countries.[11,12,38] It has been reported that common polymorphisms might modulate the activity of the primary disease-causing mutation or influence susceptibility to arrhythmia, even in the general population.[39] The common polymorphisms may attribute to ethnic differences in the clinical phenotype in inherited cardiac arrhythmias, including BS, because some common polymorphisms are ethnically dependent. Pfeufer et al reported that polymorphisms in the *SCN5A* promoter were associated with a widening of QRS duration in a cen-

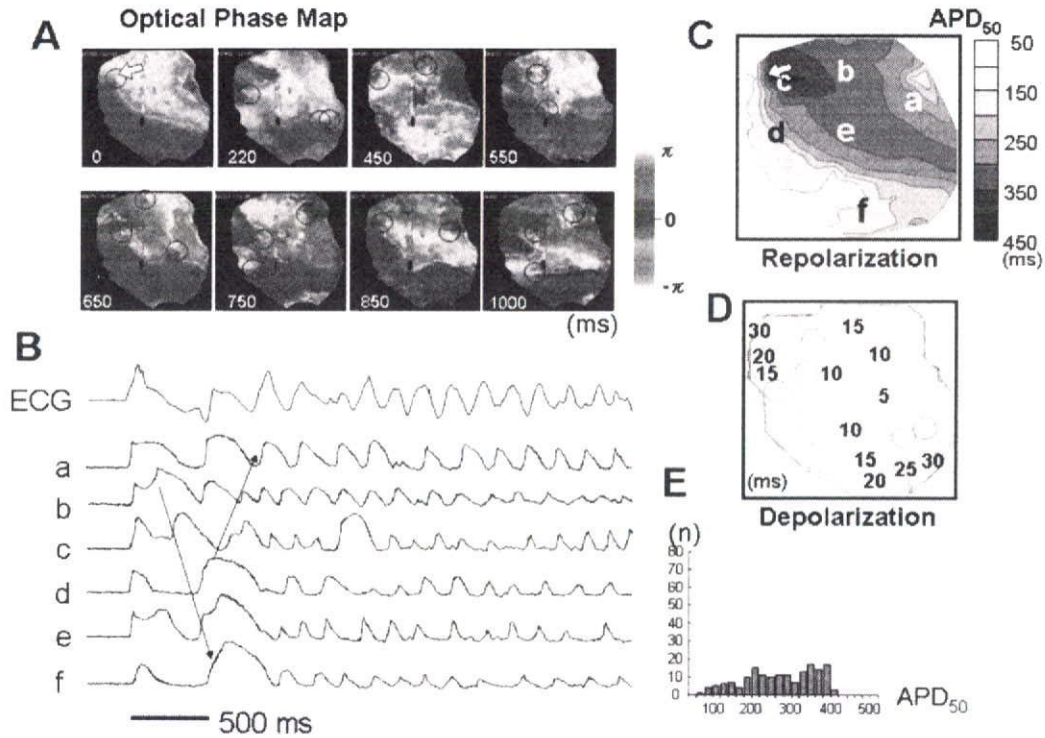

Fig 5. Mechanism underlying ventricular fibrillation (VF) in a Brugada model using a wedge preparation combined with high-resolution (256×256) optical mapping techniques. (A) Representative snapshots from a phase movie during VF originating from the epicardial (Epi) phase 2 reentry (P2R). (B) Optical action potentials at each site (a–f), together with a transmural ECG. (C, D) Repolarization and depolarization maps on the Epi surface in the condition of Brugada-ECG just before VF. (E) Epi action potential duration at 50% repolarization (APD_{50}) histogram during the first P2R-wave. The area of maximum gradient of repolarization in Epi (arrow in A and C) develops the P2R. The first P2R-wave is broken up into multiple wavelets (A, 220 ms), resulting in degeneration of ventricular tachycardia into VF. The Epi depolarization map paced from the endocardium shows a remarkable conduction delay in the episode of VF (D). The phase singularity points during the first P2R-wave (open circle in D) almost coincide with the Epi sites of delayed conduction. There is a large variety of APD in Epi during the first P2R-wave (E). Thus, P2R-extrasystoles degenerate into VF with further depolarization and repolarization disturbances. Open circles mark phase singularity points (Modified from *J Am Coll Cardiol* 2006; **47:** 2074–2085 with permission).

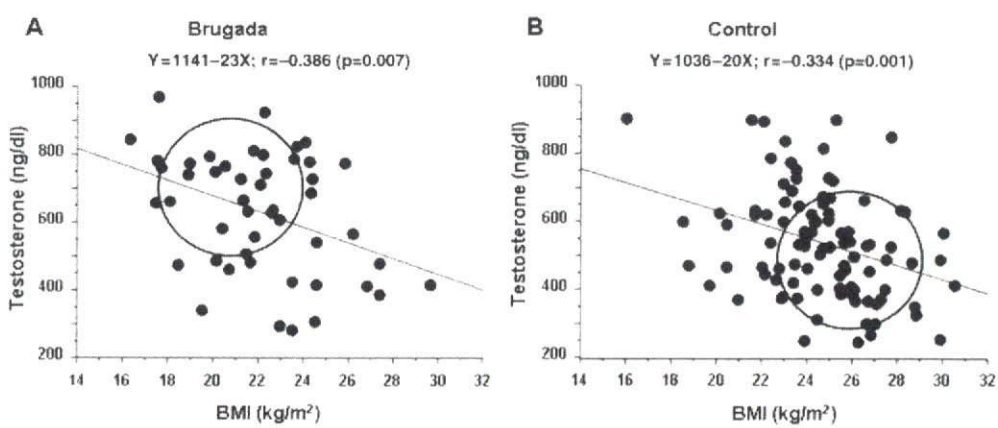

Fig 6. Correlation between testosterone level and body mass index (BMI) in Brugada syndrome males and age-matched control males. Testosterone level inversely correlated withe BMI in both groups (*J Cardiovasc Electrophysiol* 2007 (in press), with permission).

tral European general population.[40] We recently identified a haplotype variant consisting of 6 individual DNA polymorphisms in near-complete linkage disequilibrium within the proximal promoter region of *SCN5A* in Asians only (an allele frequency of 22%), not in Caucasian or African-Americans (Fig 7).[41] Luciferase reporter activity of this variant haplotype, designated Haplotype B, in cardiomyocytes is reduced 62% compared with the wild-type, designated Haplotype A. To test the hypothesis that this *SCN5A* promoter polymorphism may modulate variability in cardiac

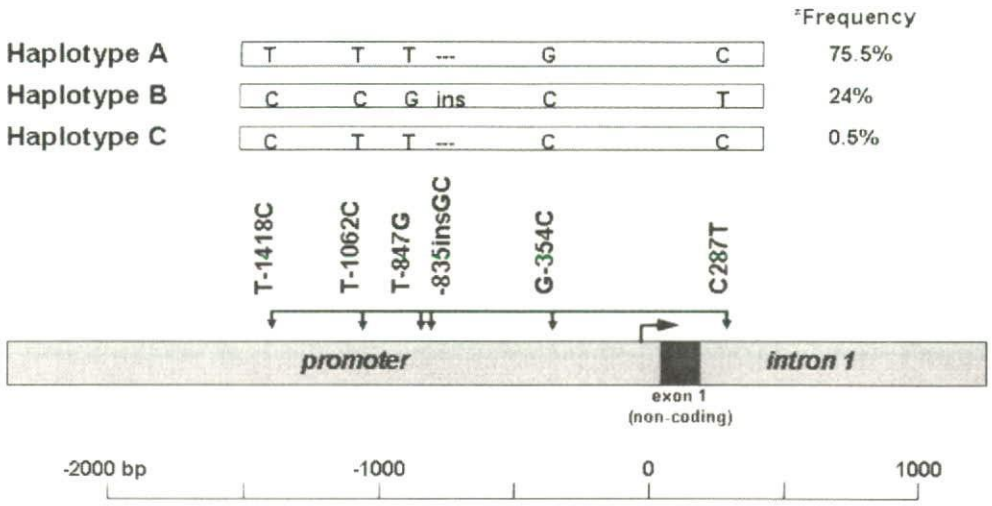

Fig 7. Haplotypes identified within the proximal promoter region of *SCN5A*, a cardiac sodium-channel gene. The 6 polymorphisms are in near-complete linkage disequilibrium. Haplotype A is designated as containing all common alleles, and Haplotype B as containing all minor alleles. The discordant haplotype is designated Haplotype C. *Frequency in the Japanese (control) population (Modified from *Circulation* 2006; **113:** 338–344 with permission).

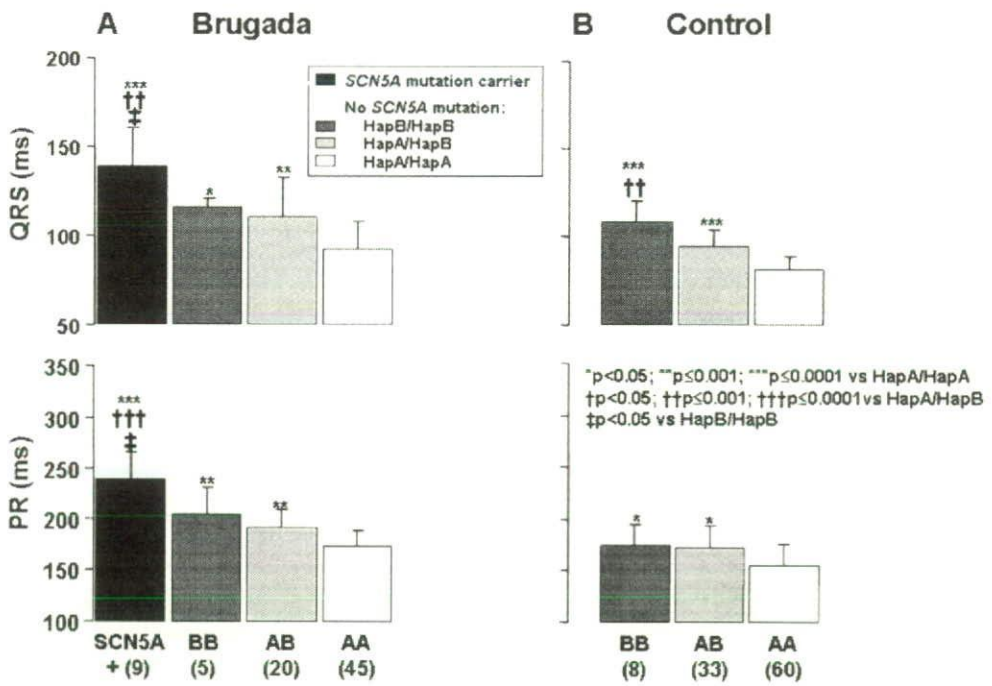

Fig 8. *SCN5A* promoter haplotype pair effects on QRS duration in lead V_6 and PR duration in lead II in patients with Brugada syndrome and in control subjects. In the Brugada patients without *SCN5A* mutations and in the control subjects, both QRS and PR duration show a gene–dose effect, being longest in Haplotype B homozygotes (BB), intermediate in Haplotype A/Haplotype B heterozygotes (AB) and shortest in Haplotype A homozygotes (AA). The Brugada patients with *SCN5A* mutations show the longer duration of both QRS and PR than do those without *SCN5A* mutations. Patient numbers are indicated between parentheses. Data mean±SD (Modified from *Circulation* 2006; **113:** 338–344 with permission).

conduction, the relationship between the *SCN5A* promoter haplotype and indices of conduction velocity (ie, PR and QRS durations) was analyzed in a cohort of 71 Japanese BS subjects without *SCN5A* mutations and in 102 Japanese controls. In both groups, PR and QRS durations were significantly longer in Haplotype B individuals, with a gene–dose effect (Fig 8). Moreover, increases in both the PR and QRS duration with sodium channel blockers, which are known to be arrhythmogenic in BS, were genotype-dependent and a gene–dose effect was also observed. These data demonstrate that the Haplotype B within the *SCN5A* promoter region alone does not give rise to BS, but that it likely contributes to a higher incidence of BS in Asian population in combination with other yet unknown (genetic) factors.

Acknowledgments

Dr W Shimizu was supported by the Uehara Memorial Foundation, the Hoansha Research Foundation, Japan Research Foundation for Clinical Pharmacology, Ministry of Education, Culture, Sports, Science and Technology Leading Project for Biosimulation, and Health Sciences Research Grants (H18-Research on Human Genome-002) from the Ministry of Health, Labour and Welfare, Japan.

References

1. Brugada P, Brugada J. Right bundle branch block, persistent ST segment elevation and sudden cardiac death: A distinct clinical and electrocardiographic syndrome: A multicenter report. *J Am Coll Cardiol* 1992; **20:** 1391–1396.
2. Alings M, Wilde A. "Brugada" syndrome: Clinical data and suggested pathophysiological mechanism. *Circulation* 1999; **99:** 666–673.
3. Antzelevitch C, Brugada P, Brugada J, Brugada R, Shimizu W, Gussak I, et al. Brugada syndrome: A decade of progress. *Circ Res* 2002; **91:** 1114–1118.
4. Priori SG, Napolitano C, Gasparini M, Pappone C, Della Bella P, Giordano U, et al. Natural history of Brugada syndrome: Insights for risk stratification and management. *Circulation* 2002; **105:** 1342–1347.
5. Wilde AA, Antzelevitch C, Borggrefe M, Brugada J, Brugada R, Brugada P, et al. Proposed diagnostic criteria for the Brugada syndrome: Consensus report. *Circulation* 2002; **106:** 2514–2519.
6. Brugada J, Brugada R, Brugada P. Determinants of sudden cardiac death in individuals with the electrocardiographic pattern of Brugada syndrome and no previous cardiac arrest. *Circulation* 2003; **108:** 3092–3096.
7. Antzelevitch C, Brugada P, Borggrefe M, Brugada J, Brugada R, Corrado D, et al. Brugada Syndrome: Report of the Second Consensus Conference: Endorsed by the Heart Rhythm Society and the European Heart Rhythm Association. *Circulation* 2005; **111:** 659–670.
8. Shimizu W, Aiba T, Kamakura S. Mechanisms of disease: Current understanding and future challenges in Brugada syndrome. *Nat Clin Pract Cardiovasc Med* 2005; **2:** 408–414.
9. Shimizu W, Matsuo K, Takagi M, Tanabe Y, Aiba T, Taguchi A, et al. Body surface distribution and response to drugs of ST segment elevation in the Brugada syndrome: Clinical implication of 87-leads body surface potential mapping and its application to 12-leads electrocardiograms. *J Cardiovasc Electrophysiol* 2000; **11:** 396–404.
10. Miyamoto K, Yokokawa M, Tanaka K, Nagai T, Okamura H, Noda T, et al. Diagnostic and prognostic value of type 1 Brugada electrocardiogram at higher (third or second) V1 to V2 recording in men with Brugada syndrome. *Am J Cardiol* 2007; **99:** 53–57.
11. Nademanee K, Veerakul G, Nimmannit S, Chaowakul V, Bhuripanyo K, Likittanasombat K, et al. Arrhythmogenic marker for the sudden unexplained death syndrome in Thai men. *Circulation* 1997; **96:** 2595–2600.
12. Atarashi H, Ogawa S, Harumi K, Sugimoto T, Inoue H, Murayama M, et al. Three-year follow-up of patients with right bundle branch block and ST segment elevation in the right precordial leads: Japanese Registry of Brugada Syndrome: Idiopathic Ventricular Fibrillation Investigators. *J Am Coll Cardiol* 2001; **37:** 1916–1920.
13. Kanda M, Shimizu W, Matsuo K, Nagaya N, Taguchi A, Suyama K, et al. Electrophysiologic characteristics and implication of induced ventricular fibrillation in symptomatic patients with Brugada syndrome. *J Am Coll Cardiol* 2002; **39:** 1799–1805.
14. Eckardt L, Probst V, Smits JP, Bahr ES, Wolpert C, Schimpf R, et al. Long-term prognosis of individuals with right precordial ST-segment-elevation Brugada syndrome. *Circulation* 2005; **111:** 257–263.
15. Shimizu W. Gender difference and drug challenge in Brugada syndrome (Editorial Comment). *J Cardiovasc Electrophysiol* 2004; **15:** 70–71.
16. Shimizu W. The long QT syndrome: Therapeutic implications of a genetic diagnosis. *Cardiovasc Res* 2005; **67:** 347–356.
17. Chen Q, Kirsch GE, Zhang D, Brugada R, Brugada J, Brugada P, et al. Genetic basis and molecular mechanisms for idiopathic ventricular fibrillation. *Nature* 1998; **392:** 293–296.
18. Weiss R, Barmada MM, Nguyen T, Seibel JS, Cavlovich D, Kornblit CA, et al. Clinical and molecular heterogeneity in the Brugada syndrome: A novel gene locus on chromosome 3. *Circulation* 2002; **105:** 707–713.
19. Antzelevitch C, Pollevick GD, Cordeiro JM, Casis O, Sanguinetti MC, Aizawa Y, et al. Loss-of-function mutations in the cardiac calcium channel underlie a new clinical entity characterized by ST-segment elevation, short QT intervals, and sudden cardiac death. *Circulation* 2007; **115:** 442–449.
20. Tan HL, Bezzina CR, Smits JP, Verkerk AO, Wilde AA. Genetic control of sodium channel function. *Cardiovasc Res* 2003; **57:** 961–973.
21. Baroudi G, Acharfi S, Larouche C, Chahine M. Expression and intracellular localization of an *SCN5A* double mutant R1232W/T1620M implicated in Brugada syndrome. *Circ Res* 2002; **90:** E11–E16.
22. Ye B, Valdivia CR, Ackerman MJ, Makielski JC. A common human SCN5A polymorphism modifies expression of an arrhythmia causing mutation. *Physiol Genomics* 2003; **12:** 187–193.
23. Litovsky SH, Antzelevitch C. Transient outward current prominent in canine ventricular epicardium but not endocardium. *Circ Res* 1988; **62:** 116–126.
24. Krishnan SC, Antzelevitch C. Flecainide-induced arrhythmia in canine ventricular epicardium: Phase 2 Reentry? *Circulation* 1993; **87:** 562–5729.
25. Yan GX, Antzelevitch C. Cellular basis for the electrocardiographic J wave. *Circulation* 1996; **93:** 372–379.
26. Yan GX, Antzelevitch C. Cellular basis for the Brugada syndrome and other mechanisms of arrhythmogenesis associated with ST segment elevation. *Circulation* 1999; **100:** 1660–1666.
27. Aiba T, Shimizu W, Hidaka I, Uemura K, Noda T, Zheng C, et al. Cellular basis for trigger and maintenance of ventricular fibrillation in the Brugada syndrome model: High resolution optical mapping study. *J Am Coll Cardiol* 2006; **47:** 2074–2085.
28. Frustaci A, Priori SG, Pieroni M, Chimenti C, Napolitano C, Rivolta I, et al. Cardiac histological substrate in patients with clinical phenotype of Brugada syndrome. *Circulation* 2005; **112:** 3680–3687.
29. Yokokawa M, Kitamura S, Okamura H, Noda T, Suyama K, Kurita T, et al. Long-term follow-up of electrocardiographic features in patients with Brugada syndrome: Comparison between *SCN5A* mutation carriers and non-mutation carriers (abstract). *Circulation* 2006; **114:** II-471.
30. Di Diego JM, Cordeiro JM, Goodrow RJ, Fish JM, Zygmunt AC, Perez GJ, et al. Ionic and cellular basis for the predominance of the Brugada syndrome phenotype in males. *Circulation* 2002; **106:** 2004–2011.
31. Shuba YM, Degtiar VE, Osipenko VN, Naidenov VG, Woosley RL. Testosterone-mediated modulation of HERG blockade by proarrhythmic agents. *Biochem Pharmacol* 2001; **62:** 41–49.
32. Liu XK, Katchman A, Whitfield BH, Wan G, Janowski EM, Woosley RL, et al. In vivo androgen treatment shortens the QT interval and increases the densities of inward and delayed rectifier potassium currents in orchiectomized male rabbits. *Cardiovasc Res* 2003; **57:** 28–36.
33. Bai CX, Kurokawa J, Tamagawa M, Nakaya H, Furukawa T. Nontranscriptional regulation of cardiac repolarization currents by testosterone. *Circulation* 2005; **112:** 1701–1710.
34. Matsuo K, Akahoshi M, Seto S, Yano K. Disappearance of the Brugada-type electrocardiogram after surgical castration: A role for testosterone and an explanation for the male preponderance. *Pacing Clin Electrophysiol* 2003; **26:** 1551–1553.
35. Glass AR, Swerdloff RS, Bray GA, Dahms WT, Atkinson RL. Low serum testosterone and sex-hormone-binding-globulin in massively obese men. *J Clin Endocrinol Metab* 1977; **45:** 1211–1219.
36. Matsuo K, Akahoshi M, Nakashima E, Seto S, Yano K. Clinical characteristics of subjects with the Brugada-type electrocardiogram: A case control study. *J Cardiovasc Electrophysiol* 2004; **15:** 653–657.
37. Shimizu W, Matsuo K, Kokubo Y, Satomi K, Kurita T, Noda T, et al. Sex hormone and gender difference--role of testosterone on male predominance in Brugada syndrome. *J Cardiovasc Electrophysiol* 2007; **18:** 415–421.
38. Vatta M, Dumaine R, Varghese G, Richard TA, Shimizu W, Aihara N, et al. Genetic and biophysical basis of sudden unexplained nocturnal death syndrome (SUNDS), a disease allelic to Brugada syndrome. *Hum Mol Genet* 2002; **11:** 337–345.
39. Splawski I, Timothy KW, Tateyama M, Clancy CE, Malhotra A, Beggs AH, et al. Variant of SCN5A sodium channel implicated in risk of cardiac arrhythmia. *Science* 2002; **297:** 1333–1336.
40. Pfeufer A, Jalilzadeh S, Perz S, Mueller JC, Hinterseer M, Illig T, et al. Common variants in myocardial ion channel genes modify the QT interval in the general population: Results from the KORA study. *Circ Res* 2005; **96:** 693–701.
41. Bezzina CR, Shimizu W, Yang P, Koopmann TT, Tanck MWT, Miyamoto Y, et al. A common sodium channel promoter haplotype in Asian subjects underlies variability in cardiac conduction. *Circulation* 2006; **113:** 338–344.

Clinical Aspects of Type-1 Long-QT Syndrome by Location, Coding Type, and Biophysical Function of Mutations Involving the KCNQ1 Gene

Arthur J. Moss, MD*; Wataru Shimizu, MD, PhD*; Arthur A.M. Wilde, MD, PhD*; Jeffrey A. Towbin, MD*; Wojciech Zareba, MD, PhD; Jennifer L. Robinson, MS; Ming Qi, PhD; G. Michael Vincent, MD; Michael J. Ackerman, MD, PhD; Elizabeth S. Kaufman, MD; Nynke Hofman, MSc; Rahul Seth, MD; Shiro Kamakura, MD, PhD; Yoshihiro Miyamoto, MD, PhD; Ilan Goldenberg, MD; Mark L. Andrews, BBA; Scott McNitt, MS

Background—Type-1 long-QT syndrome (LQTS) is caused by loss-of-function mutations in the KCNQ1-encoded I_{Ks} cardiac potassium channel. We evaluated the effect of location, coding type, and biophysical function of KCNQ1 mutations on the clinical phenotype of this disorder.

Methods and Results—We investigated the clinical course in 600 patients with 77 different KCNQ1 mutations in 101 proband-identified families derived from the US portion of the International LQTS Registry (n=425), the Netherlands' LQTS Registry (n=93), and the Japanese LQTS Registry (n=82). The Cox proportional hazards survivorship model was used to evaluate the independent contribution of clinical and genetic factors to the first occurrence of time-dependent cardiac events from birth through age 40 years. The clinical characteristics, distribution of mutations, and overall outcome event rates were similar in patients enrolled from the 3 geographic regions. Biophysical function of the mutations was categorized according to dominant-negative (>50%) or haploinsufficiency (≤50%) reduction in cardiac repolarizing I_{Ks} potassium channel current. Patients with transmembrane versus C-terminus mutations (hazard ratio, 2.06; $P<0.001$) and those with mutations having dominant-negative versus haploinsufficiency ion channel effects (hazard ratio, 2.26; $P<0.001$) were at increased risk for cardiac events, and these genetic risks were independent of traditional clinical risk factors.

Conclusions—This genotype–phenotype study indicates that in type-1 LQTS, mutations located in the transmembrane portion of the ion channel protein and the degree of ion channel dysfunction caused by the mutations are important independent risk factors influencing the clinical course of this disorder. (***Circulation*****. 2007;115:2481-2489.)**

Key Words: electrocardiography ■ genetics ■ long-QT syndrome

The hereditary long-QT syndrome (LQTS) is characterized by prolonged ventricular repolarization on the ECG and arrhythmia-related syncope and sudden death.[1] Mutations in 1 or more of several ion channel genes are known to cause this disorder,[2] with mutations in the KCNQ1 gene causing the type-1 long-QT syndrome.[3,4] The KCNQ1 gene codes for the potassium channel protein responsible for the slow component of the delayed rectifier repolarizing current (I_{Ks}). Mutations involving this gene result in reduction of the repolarizing I_{Ks} current and lengthening of the QT interval.[3]

Clinical Perspective p 2489

Functional I_{Ks} channels result from the coassembly of 4 subunits into a tetrameric protein channel that is transported to the myocyte membrane. Each subunit contains 6 membrane-spanning domains (S1 to S6) flanked by amino (N)- and carboxyl (C)-terminus regions. Two distinct biophysical mechanisms mediate the reduced I_{Ks} current in patients with KCNQ1 mutations: (1) coassembly or trafficking defects in which mutant subunits are not transported

Received September 17, 2006; accepted March 2, 2007.

From the Cardiology Division (A.J.M., W.Z., J.L.R., I.G., M.L.A., S.M., R.S.) of the Department of Medicine and the Department of Pathology (M.Q.), University of Rochester School of Medicine and Dentistry, Rochester, NY; Division of Cardiology, Department of Internal Medicine (W.S., S.K.) and Laboratory of Molecular Genetics (Y.M.), National Cardiovascular Center, Suita, Japan; Departments of Clinical and Experimental Cardiology (A.A.M.W.) and Clinical Genetics (N.H.), Academic Medical Center, Amsterdam, the Netherlands; Department of Pediatrics, Baylor College of Medicine, Texas Children's Hospital, Houston (J.A.T.); School of Medicine, University of Utah, Salt Lake City (G.M.V.); Departments of Medicine, Pediatrics, and Molecular Pharmacology, Mayo Clinic College of Medicine, Rochester, Minn (M.J.A.); and Heart and Vascular Research Center, MetroHealth Campus of Case Western Reserve University, Cleveland, Ohio (E.S.K.).

*The first 4 authors contributed equally to this work.

The online-only Data Supplement, consisting of references, is available with this article at http://circ.ahajournals.org/cgi/content/full/CIRCULATIONAHA.106.665406/DC1.

Correspondence to Arthur J. Moss, MD, Heart Research Follow-Up Program, Box 653, University of Rochester Medical Center, Rochester, NY 14642-8653. E-mail heartajm@heart.rochester.edu

Circulation **is available at http://www.circulationaha.org** **DOI: 10.1161/CIRCULATIONAHA.106.665406**

properly to the cell membrane and fail to incorporate into the tetrameric channel, with the net effect being a ≤50% reduction in channel function (haploinsufficiency)[5]; and (2) formation of defective channels involving mutant subunits with the altered channel protein transported to the cell membrane, resulting in a dysfunctional channel having >50% reduction in channel current (dominant-negative effect).[6]

Limited prior studies involving relatively small numbers of patients with type-1 LQTS have been reported with conflicting results on the relationship between various KCNQ1 mutations and the clinical outcome.[7,8] We hypothesized that the location, coding type, and functional effect of the channel mutation would have important influence on the phenotypic manifestations and clinical course of patients with this disorder. To test this hypothesis, we investigated the clinical aspects of a large cohort of subjects having a spectrum of KCNQ1 mutations categorized by their location, coding type, and type of biophysical ion channel dysfunction.

Methods

Study Population

The study population of 600 subjects with genetically confirmed KCNQ1 mutations was derived from 101 proband-identified families with the type-1 LQTS disorder. The proband in each family had QTc prolongation not due to a known cause. The subjects were drawn from the US portion of the International LQTS Registry (n=425), the Netherlands' LQTS Registry (n=93), and the Japanese LQTS Registry (n=82). All subjects or their guardians provided informed consent for the genetic and clinical studies.

Phenotype Characterization

Routine clinical and ECG parameters were acquired at the time of enrollment in each of the registries. Follow-up was censored at age 41 years to avoid the influence of coronary disease on cardiac events. Measured parameters on the first recorded ECG included QT and R-R intervals in milliseconds, with QT corrected for heart rate by Bazett's formula. The QTc interval was expressed in its continuous form and categorized into 3 levels: <500, 500 to 530, and >530 ms. Clinical data were collected on prospectively designed forms with information on demographic characteristics, personal and family medical history, ECG findings, therapy, and end points during long-term follow-up. LQTS-related cardiac events included syncope, aborted cardiac arrest, or unexpected sudden death without a known cause. Data common to all 3 LQTS registries involving genetically identified patients with type-1 genotype were electronically merged into a common database for the present study.

Genotype Characterization

The KCNQ1 mutations were identified with the use of standard genetic tests performed in academic molecular-genetic laboratories including the Functional Genomics Center, University of Rochester Medical Center, Rochester, NY; Baylor College of Medicine, Houston, Tex; Mayo Clinic College of Medicine, Rochester, Minn; Boston Children's Hospital, Boston, Mass; Laboratory of Molecular Genetics, National Cardiovascular Center, Suita, Japan; and Department of Clinical Genetics, Academic Medical Center, Amsterdam, Netherlands.

Genetic alterations of the amino acid sequence were characterized by location and by the specific mutation (missense, splice site, in-frame insertions/deletions, nonsense, stop codon, and frameshift). The transmembrane region of the KCNQ1-encoded channel was defined as the coding sequence involving amino acid residues from 120 through 355 (S5-pore-S6 region 285 to 355), with the N-terminus region defined before residue 120 and the C-terminus region after residue 355. Nineteen study patients had intron mutations predicted to disrupt the canonical splice-site domains. Fifty-one subjects died of sudden cardiac death at a young age but did not have genotype studies. These 51 subjects were assumed to have the same KCNQ1 mutation as other affected members of their respective family. Twelve subjects had 2 mutations, one in the KCNQ1 gene and a second mutation in another LQTS ion channel gene; these 12 subjects are described separately and are not included in any of the tables or outcome analyses. Subjects with Jervell and Lange-Nielsen syndrome with deafness and 2 KCNQ1 mutations as well as those with 1 known KCNQ1 mutation and congenital deafness are not included in the present study.

The biophysical function of the mutant channels was classified as having dominant-negative effect (>50% reduction in function) or haploinsufficiency (≤50% reduction in function) on the basis of the following: (1) cellular expression studies for those with missense (n=21) and nonsense (n=2) mutations reported in the literature, with the functional information derived exclusively from heterologous expression studies; and (2) assumed loss of function for identified nonsense, splice site, in-frame deletion, and frameshift mutations (n=10) that have not yet been functionally characterized. Forty-one missense mutations and the 3 intron mutations that have not been functionally reported in cellular expression studies were categorized as unknown in terms of type of functional perturbation.

Statistical Analysis

Differences in the univariate characteristics by specific groupings were evaluated by standard statistical methods. The primary end point was time to syncope, aborted cardiac arrest, or sudden death, whichever occurred first. The cumulative probability of a first cardiac event was assessed by the Kaplan-Meier method with significance testing by the log-rank statistic. The Cox proportional hazards survivorship model was used to evaluate the independent contribution of clinical and genetic factors to the first occurrence of time-dependent cardiac events from birth through age 40 years.[9] Stratified and unstratified Cox regression models, allowing for time-dependent covariates, were fit to estimate the adjusted hazard ratio of each factor as a predictor of first cardiac events. We observed that sex was not proportional as a function of age with crossover in risk at age 13 years on univariate Kaplan-Meier analysis. To relax the assumption of proportional hazards for sex over the entire age range, separate nonparametric baseline hazard functions were allowed for male and female subjects via the stratified Cox model; then, to summarize the sex effect, sex was modeled in an unstratified Cox model as a time-dependent covariate (via an interaction with time), allowing for different hazard ratios by sex before and after age 13 years.

Because almost all the subjects were first- and second-degree relatives of probands, the effect of lack of independence between subjects was evaluated in the Cox model with grouped jackknife estimates for family membership.[10] All grouped jackknife standard errors for the covariate risk factors fell within 3% of those obtained from the unadjusted Cox model, and therefore only the Cox model findings are reported.

Patients who died suddenly at a young age from suspected LQTS and who did not have an ECG for QTc measurement were identified in the Cox models as "QTc missing." Prespecified covariate interactions were evaluated. The influence of time-dependent β-blocker therapy (the age at which β-blocker therapy was initiated) on outcome was determined by adding this variable to the final Cox model containing the various covariates.

The authors had full access to and take full responsibility for the integrity of the data. All authors have read and agree to the manuscript as written.

Results

Total Study Population

The spectrum and number of KCNQ1 mutations by location, type of mutation, and functional effect are presented in Table 1, with the location frequency of the mutations presented diagrammatically in Figure 1. A total of 77 different KCNQ1

TABLE 1. KCNQ1 Mutations by Location and Coding, Type of Mutation, and Functional Effect

Location and Coding*	No. of Subjects†	Type of Mutation	Functional Effect‡
N-terminus			
M1V	1	Missense	Unknown
G57V	1	Missense	Unknown
Transmembrane			
W120C	2	Missense	Unknown
T144A	7	Missense	Unknown
A150fs/133 [del CT 451-452]	2	Frameshift	Haploinsufficiency
E160K	3	Missense	Unknown
G168R	44	Missense	Unknown
Y171X [513 C>G]	6	Nonsense	Haploinsufficiency
R174H	2	Missense	Unknown
A178P	5	Missense	Dominant-negative effect (a)
Y184S	18	Missense	Unknown
G185S	10	Missense	Unknown
G189E	2	Missense	Unknown
G189R	4	Missense	Dominant-negative effect (b)
R190Q	4	Missense	Haploinsufficiency (b, c)
L191fs/90 [del TGCGC 572-576]	8	Frameshift	Haploinsufficiency
R195fs/40 [del G 585]	2	Frameshift	Haploinsufficiency
S225L	13	Missense	Dominant-negative effect (d)
A226V	3	Missense	Unknown
R237P	1	Missense	Unknown
D242N	3	Missense	Unknown
R243C	13	Missense	Haploinsufficiency (e)
V254 mol/L	59	Missense	Dominant-negative effect (b, f)
R258C	1	Missense	Haploinsufficiency
R259C	1	Missense	Haploinsufficiency (g)
L266P	15	Missense	Unknown
G269D	35	Missense	Dominant-negative effect (h)
G269S	25	Missense	Haploinsufficiency (i)
L273F	6	Missense	Dominant-negative effect (a)
I274V	1	Missense	Unknown
S277L	3	Missense	Unknown
Y278H	2	Missense	Unknown
E284K	2	Missense	Unknown
G292D	3	Missense	Unknown
F296S	2	Missense	Unknown
G306R	2	Missense	Dominant-negative effect (b, j)
V310I	1	Missense	Unknown
T312I	14	Missense	Dominant-negative effect (a)
G314S	8	Missense	Dominant-negative effect (h, k, l, m)
Y315C	10	Missense	Dominant-negative effect (d, n)
Y315S	1	Missense	Dominant-negative effect (h, m)
D317G	3	Missense	Unknown
P320H	1	Missense	Unknown
T322 mol/L	2	Missense	Unknown
G325R	3	Missense	Unknown
delF340 [del CTT 1017-1019]	7	In-frame deletion	Haploinsufficiency
A341E	9	Missense	Dominant-negative effect (b)
A341V	20	Missense	Dominant-negative effect (o)

TABLE 1. Continued

Location and Coding*	No. of Subjects†	Type of Mutation	Functional Effect‡
P343S	1	Missense	Dominant-negative effect (p)
A344A/sp [1032 G>A]	27	Splice site	Haploinsufficiency
A344V	17	Missense	Unknown
S349W	15	Missense	Unknown
L353P	4	Missense	Unknown
C-terminus			
Q357H	3	Missense	Unknown
R360G	3	Missense	Unknown
S373P	7	Missense	Unknown
K393N	10	Missense	Unknown
R397W	5	Missense	Unknown
P400fs/62 [ins C 1201-1022]	6	Frameshift	Haploinsufficiency
P448fs/13 [ins G 1344-1345]	11	Frameshift	Haploinsufficiency
I517T	3	Missense	Unknown
R518X [1552 C>T]	11	Nonsense	Haploinsufficiency (q)
M520R	3	Missense	Unknown
V524G	4	Missense	Unknown
Q530X [1588 C>T]	13	Nonsense	Haploinsufficiency (q)
R562 mol/L	2	Missense	Unknown
S566F	3	Missense	Unknown
I567S	6	Missense	Unknown
S571fs/20 [del C 1714]	3	Frameshift	Haploinsufficiency
R591C	5	Missense	Unknown
R591H	6	Missense	Haploinsufficiency (r)
R594Q	11	Missense	Haploinsufficiency (q)
D611Y	10	Missense	Haploinsufficiency (s)
A636fs/28 [del C 1909]	2	Frameshift	Haploinsufficiency
Intron			
IVS2+1 G>A	2	Splice site	Unknown
IVS4+5 G>A	2	Splice site	Unknown
IVS7+5 G>A	15	Splice site	Unknown

*The numbers and letters refer to the amino acid coding of the mutant channel protein. The brackets contain the nucleotide code for deletions, frameshift, splice site, and nonsense mutations.

†Included in this table are 52 subjects who died suddenly at a young age. These subjects were from families with a known KCNQ1 mutation and were assumed to have their respective family mutation.

‡Dominant-negative effect is associated with >50% reduction whereas haploinsufficiency is associated with ≤50% reduction in ion channel repolarizing current. See text for details. Letters in parentheses refer to references that are available in the online-only Data Supplement.

mutations were identified. A majority of the mutations were localized to the S1 to S6 transmembrane domains (66%), and missense (single amino acid substitutions) accounted for 81% of all the mutations.

The phenotypic characteristics of patients enrolled in each of the 3 registries and by location and type of mutation are presented in Table 2. The clinical characteristics of the patients were similar among the 3 registries except for QTc duration and frequency of β-blocker use. The QTc interval was longer and cardiac events and β-blocker use were more frequent in patients with mutations in the transmembrane than in the C-terminus location. β-Blockers were used less frequently in patients from the Japanese registry than in patients from the other 2 registries. The frequency of first cardiac events was higher in those with than without missense mutations. The clinical characteristics of the 19 subjects possessing intron mutations resembled those with transmembrane and missense mutations.

The QTc interval was significantly longer in the 12 patients with 2 mutations than in those with only single KCNQ1 mutations (570±70 versus 480±60 ms; $P<0.01$). All 12 patients with 2 mutations experienced at least 1 cardiac event.

The cumulative probabilities of first cardiac event by location and type of mutation are presented in Figure 2A and 2B, respectively. Significantly higher event rates were found in subjects with transmembrane than C-terminus mutations and in those with than without missense mutations, with the most rapid increase in event rates occurring during ages 7 to

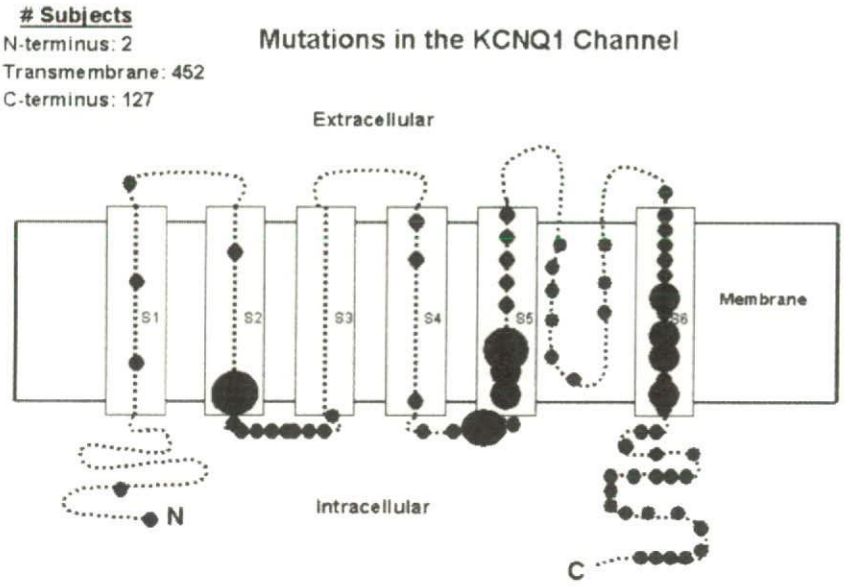

Figure 1. Frequency and location of 74 different mutations in the KCNQ1 potassium channel involving 581 subjects. The 19 subjects with 3 intron mutations are not included in this diagram. The α subunit involves the N-terminus (N), 6 membrane-spanning segments, and the C-terminus portion (C). The size of the circles reflect the number of subjects with mutations at the respective locations, with the small circles indicating <15, medium-sized circles 15 to 30, and large circles >30 subjects.

20 years. In patients with transmembrane-localized mutations, the event rates for patients with mutations localized to the pore region (S5-pore-S6) were nearly identical to those with nonpore mutations (data not shown).

The findings from the Cox regression analysis for location and type of mutation are presented in Table 3. The clinical risk factors associated with first cardiac events involved males before age 13 years, females after age 13

TABLE 2. Phenotypic Characteristics by Source of Subjects, Location of Mutation, and Type of Mutation

	Source of Subjects			Location of Mutation		Missense Mutation		
Characteristics	United States (n=425)	Netherlands (n=93)	Japan (n=82)	Trans Membrane (n=452)	C-Terminus (n=127)	Yes (n=483)	No (n=98)	Intron Mutation (n=19)
Female, %	57	53	54	57	51	54	62	63
ECG at enrollment								
QTc††, ms	488±58	450±45	472±46	485±53	460±61	481±59	471±38	478±60
Therapy, %								
β-Blockers†‡	45	34	26	45	28	42	38	37
Pacemaker	2.4	0	0	1.5	2.4	1.4	3.1	0
Sympathectomy	0.5	0	0	0.4	0	0.4	0	0
Defibrillator	6.4	3.2	0	5.8	3.1	5.2	5.1	0
First cardiac event*‡§, %	41	37	38	45	21	43	26	42
Syncope‡ (n=200)	35	31	29	38	17	36	21	32
Aborted cardiac arrest (n=15)	1.9	1.1	7.3	2.9	0.8	2.5	2.0	5.3
Death (n=23)	4.0	5.5	1.2	4.0	3.1	4.2	2.0	5.3
Ever cardiac event, %								
Syncope‡§	35	31	31	39	17	37	21	33
Aborted cardiac arrest†	2.4	15	8.8	5.3	3.2	5.4	2.0	11
Death	11	14	2.4	10	6.3	11	4.1	26

Plus-minus values are mean±SD. Percentages >10 are rounded to a whole number. The 600 subjects in this table include 51 subjects who died suddenly at a young age, were from families with known KCNQ1 mutation, and were assumed to have the family mutation. Patients with intron mutations are categorized separately and are not included in the location or missense categories. Seven subjects with transmembrane mutations and 1 with C-terminus mutations had missing data about the date of the first cardiac event. Eight subjects with missense mutations had missing data about the date of the first cardiac event. Numbers in parentheses indicate the total number of specific first cardiac events from the 3 sources of patients.

*First cardiac event was syncope, aborted cardiac arrest, or sudden death, whichever occurred first.

†$P<0.01$ for the comparison of characteristics among the 3 sources of subjects.

‡$P<0.01$ for the comparison of characteristics between the 2 locations of the mutations.

§$P<0.01$ for the comparison of characteristics between missense yes and no.

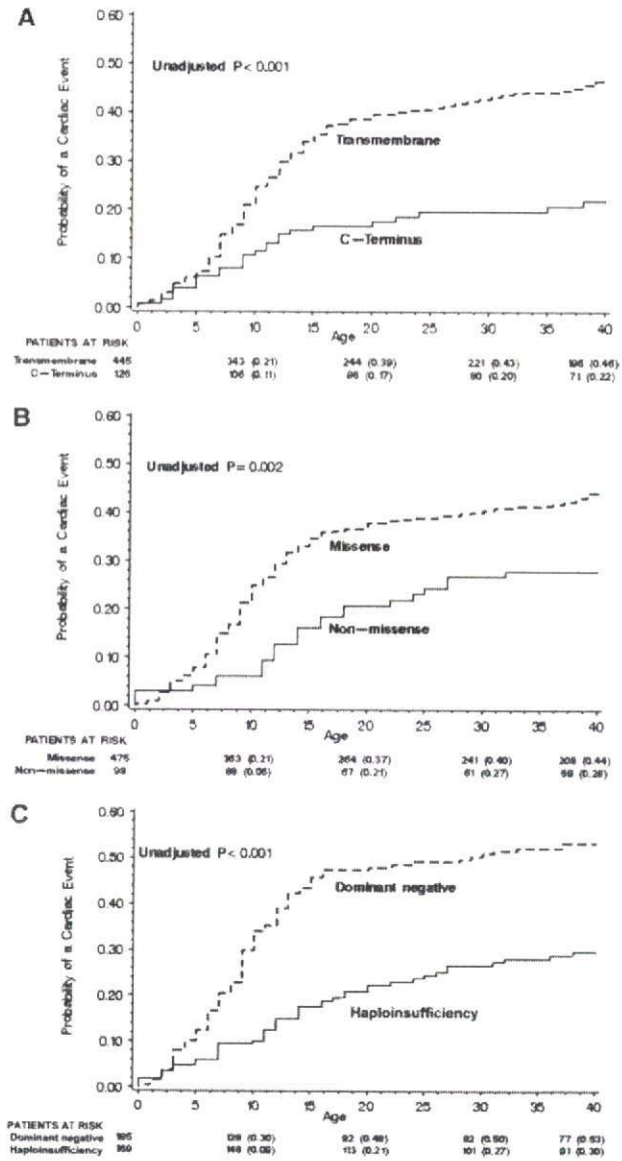

Figure 2. Kaplan-Meier estimate of the cumulative probability of a first cardiac event by location (A), type (B), and biophysical function of the mutation (C).

years, and longer QTc intervals. Mutations located in the transmembrane region of the channel made significant and independent contributions to the risk model, but missense mutations were not an independent risk factor. Three different intron mutations were present in 19 subjects from 4 families, and these intron mutations made a meaningful but nonsignificant contribution to the risk model. Prespecified interactions were investigated for their effect on cardiac events, and no significant interactions were found for transmembrane location by type of mutation, transmembrane location by QTc, or mutation type by QTc. Time-dependent β-blocker use was associated with a significant 74% reduction in the risk of first cardiac events ($P<0.001$).

TABLE 3. Cox Regression With Multiple Predictor Variables Including Location and Type of Mutations for First Cardiac Event

Variable	Hazard Ratio	95% CI	*P*
Netherlands:United States	1.15	0.74–1.78	0.55
Japan:United States	1.45	0.98–2.16	0.07
Male <13 y:female <13 y	1.72	1.25–2.38	<0.001
Female 13–40 y:male 13–40 y	2.27	1.30–3.96	<0.01
QTc 500–530 ms:QTc <500 ms	2.04	1.41–2.96	<0.001
QTc >530 ms:QTc <500 ms	3.25	2.25–4.69	<0.001
QTc missing*:QTC <500 ms	2.26	1.57–3.25	<0.001
Transmembrane:C-terminus	2.06	1.36–3.12	<0.001
Missense yes:no	1.33	0.86–2.05	0.20
Intron:C-terminus	2.45	0.98–6.11	0.06
Time-dependent β-blocker use	0.26	0.14–0.49	<0.001

The Cox analysis involved 592 subjects with 445 transmembrane, 126 C-terminus, 2 N-terminus, and 19 intron mutations; 8 subjects were not included in this Cox analysis because of missing data about the date of their first cardiac event.

*QTc missing category involves 47 subjects who died suddenly at a young age without a prior ECG.

Biophysical Function and Outcome

The clinical implications of disordered biophysical function of the mutant KCNQ1 channels were investigated in a subset of 356 subjects with known or suspected alteration in ion channel function (see Methods for functional categorization). The clinical characteristics of patients with dominant-negative and haploinsufficiency ion channel dysfunction are presented in Table 4. Patients with mutations having dominant-negative ion current effects had a longer QTc interval and a higher frequency of cardiac events than subjects with mutations resulting in haploinsufficiency. The cumulative probabilities of a first cardiac event by the biophysical function of the mutations are presented in Figure 2C. As shown in Table 5, patients with mutations having

TABLE 4. Phenotypic Characteristics by Biophysical Function of the KCNQ1 Mutations in 356 Subjects

Characteristics	Dominant-Negative Effect (n=187)	Haploinsufficiency (n=169)
Female, %	51	61
ECG at enrollment		
QTc,* ms	500±60	470±50
Therapy, %		
β-Blockers	47	37
Pacemaker	1.1	4.1
Sympathectomy	0.5	0
Defibrillator	4.8	7.7
First cardiac event*, %	53	27
Syncope	45	22
Aborted cardiac arrest	2.1	3.0
Death	5.3	2.4

Percentages >10 are rounded to a whole number. Two subjects had missing data about the date of their first cardiac event.

*$P<0.01$.

TABLE 5. Cox Regression With Multiple Predictor Variables Including Ion Channel Dysfunction for First Cardiac Events

Variable	Hazard Ratio	95% CI	P
Netherlands:United States	2.78	1.48-5.23	<0.01
Japan:United States	1.63	1.02-2.63	0.04
Male <13 y:female <13 y	1.94	1.29-2.91	<0.01
Female 13-40 y:male 13-40 y	1.95	0.99-3.87	0.06
QTc 500–530 ms:QTc <500 ms	1.88	1.18-2.99	<0.01
QTc >530 ms:QTc <500 ms	3.22	2.06-5.05	<0.001
QTc missing*:QTc <500 ms	2.07	1.29-3.33	<0.01
Dominant-negative:haploinsufficiency	2.26	1.56-3.25	<0.001
Time-dependent β-blocker use	0.21	0.09-0.48	<0.001

The analysis involved 354 subjects with known or suspected ion channel dysfunction; 2 subjects were not included because of missing data about the date of their first cardiac event.

*The QTc missing category involves 26 patients who died suddenly at a young age without a prior ECG.

dominant-negative functional effects experienced a significantly greater risk for cardiac events than those with haploinsufficiency (hazard ratio, 2.26; 95% CI, 1.56 to 3.25; $P<0.001$) after adjustment for relevant covariates including QTc and gender effects by age group. β-Blocker use was associated with a significant 79% reduction in first cardiac events in this subset of patients. Because substantial colinearity exists for transmembrane mutations, missense mutations, and mutations with dominant-negative biophysical function, the individual effects of these 3 mutation parameters could not be ascertained reliably in the same Cox model.

Discussion

The main results of the present study from 600 patients having a spectrum of KCNQ1 mutations derived from 3 LQTS registries are significantly higher cardiac event rates in patients with transmembrane mutations and in patients with mutations having a putative dominant-negative effect on the repolarizing I_{Ks} current. The effect of these genetically determined factors is independent of traditional clinical risk factors and of β-blocker therapy.

Since 1995, when the first 2 genes responsible for LQTS were identified,[11,12] molecular genetic studies have revealed a total of 9 forms of congenital LQTS caused by mutations in genes involving potassium channel (LQT-1, -2, -5, -6, and -7), sodium channel (LQT-3, -9), and calcium channel proteins (LQT-8) as well as a membrane-adapter protein (LQT-4).[2,13] Genotype–phenotype studies have enabled us to stratify risk and to treat more specifically patients with LQT-1, LQT-2, and LQT-3 subtypes of this genetic disorder. LQT-1, the most common form of LQTS, accounts for ≈50% of genotyped patients[4,14] and has more variable expressivity and incomplete penetrance than the other forms.[15] Mutation location and knowledge of the functional effects of the mutation provide additional risk information beyond the clinical risk factors and the genotype, at least for LQT-1, and this information should contribute to improved risk stratification and more focused management of these higher-risk patients.

Mutations in KCNQ1 are responsible for defects in the slowly activating component of the delayed rectifier current I_{Ks}.[16] This current is the main repolarizing current at increased heart rate and is highly sensitive to catecholamines.[3] We speculate that I_{Ks} channels with transmembrane mutations might have reduced responsiveness to the regulatory β-adrenergic signaling of the ion-conduction pathway with more impairment of shortening of the QTc with exercise-related tachycardia than mutations in the C-terminus region.

Functional I_{Ks} channels result from the coassembly of 4 KCNQ1-encoded subunits. A mutated gene encodes a protein with aberrant function, and the presence of both normal and abnormal proteins in the ion channel contributes to a >50% reduction in ion channel function (dominant-negative effect). An alternative mechanism of reduced repolarizing KCNQ1 K^+ current is the inability of mutated subunits to coassemble with normal gene products, such as occurs with a trafficking defect, resulting in a ≤50% reduction in channel function (haploinsufficiency). With only 1 exception,[17] this is the case for all studied truncating mutations leading to incomplete proteins. Our assumption that truncated proteins (based on frameshift nonsense mutations) lead to haploinsufficiency seems justified. The biophysical effect of missense mutations is unpredictable, and both haploinsufficiency and dominant-negative effects have been described. In the absence of reported biophysical studies, missense mutations were classified as unknown.

Previous attempts to identify a genotype–phenotype relationship for KCNQ1 mutations failed to reach consensus on the clinical outcome of the type and site of mutations.[7,8] Relatively small numbers and different ethnic background of the previously reported patients with the LQT-1 genotype might be responsible for the discrepant results. The present larger study allows us to demonstrate for the first time that the biophysical effect clearly affects the clinical outcome (ie, dominant-negative mutations are associated with a more severe phenotype than are mutations conferring haploinsufficiency [Figure 2C], even after adjustment for relevant covariates [Table 5]). The risk observed in 19 subjects with 3 different intron mutations was not quite significant ($P=0.06$), possibly because of small numbers, but the magnitude of the risk effect was similar to the risk accompanying transmembrane mutations. Although these intron mutations produced splice-site alterations predicted to affect the transmembrane portion of the ion channel, we used a separate categorization of intron mutations in view of the limited understanding of the structural alterations and functional effects resulting from these exon-skipping intron mutations.

A few additional findings from this large genotype–phenotype study of type-1 LQTS patients emphasize high risk for first cardiac events during adolescence, a crossover in risk by sex at approximately age 13 years, and a lower rate of first cardiac events in the adult years than in the younger years. These findings are not especially new,[18,19] but the present study highlights their presence in type-1 LQTS.

Study Limitations

The present study used the biophysical function of mutations reported in the literature in only a portion of the mutations

that were included (see references associated with Table 1 in the online-only Data Supplement). The published studies were from many different laboratories with the use of different cellular heterologous expression systems involving *Xenopus* oocytes and other cells at both room and physiological temperatures. Although such nonuniform testing may have contributed to some inconsistency in the categorized biophysical function, the finding of a significantly higher event rate in mutations with dominant-negative than with haploinsufficient effects (hazard ratio, 2.26; $P<0.001$) is unlikely to have resulted from the nonuniform testing. Unfortunately, we did not have the resources to perform such uniform testing in all 77 mutations presented in the present study.

Once a mutation was identified in KCNQ1, thorough genetic sequencing was not performed routinely in all the ion channel genes to look for second mutations. Thus, some of the patients included in the analysis may have had a second mutation in addition to the identified KCNQ1 mutation. It is estimated that ≈10% of genotype LQTS patients may carry a second mutation, and those with >1 mutation could contribute to some of the findings in our study. In addition, it is possible that some of the reported mutations (Table 1) are simply uncommon sequence mutations, but this is relatively unlikely because all the subjects in the present study were derived from families in which the proband had QTc prolongation not due to a known cause.

The outcome analyses included subjects from families with a known KCNQ1 mutation who died suddenly and unexpectedly at a young age and were classified as LQTS-related death with the same mutation that was present in the family. It is possible that a few of these subjects could have died from a non-LQTS cause or had an LQTS mutation different from the family mutation, but we think the error rate is likely to be small. The number of deaths and aborted cardiac arrest events is small, and there is insufficient power to evaluate the risk association of the genotype characteristics with these endpoint events in a multivariate time-dependent model.

Conclusions

The present study confirms that in patients with type-1 LQTS, longer QTc intervals are associated with higher cardiac event rates and that male patients are generally younger than female patients at first cardiac events.[20,21] The new findings from the present study are that transmembrane mutations and mutations with dominant-negative functional effect adversely influence the outcome of this disorder independent of traditional clinical risk factors and β-blocker therapy. The present study was not designed to assess the effectiveness of different therapies in patients with KCNQ1 mutations. The findings presented do not provide justification for using specific genotype characteristics to identify patients for implanted defibrillator therapy.

Note Added in Proof

After this article was accepted for publication, we noted the recent article by Tsuji et al, in which the A344A/sp [1032G>A] mutation that we categorized as haploinsufficient (Table 1) was reported to have a weak dominant-negative effect.[22] We reran the KCNQ1 data recategorizing the 27 A344A/sp [1032 G>A] mutations as dominant-negative. Negligible changes occurred in the results as presented in Table 5 and Figure 2C; the hazard ratio for dominant-negative:haploinsufficiency (Table 5) was unchanged at 2.26 ($P<0.001$).

Acknowledgment

We thank David J. Tester, Senior Research Technologist, Sudden Death Genomics Laboratory, Mayo Clinic College of Medicine, Rochester, Minn, for the detailed review and assistance he provided on the terminology and nomenclature for the annotated mutations presented in Table 1.

Sources of Funding

This study was supported in part by (1) research grants HL-33843 and HL-51618 from the National Institutes of Health, Bethesda, Md (Dr Moss); (2) Ministry of Education, Culture, Sports, Science, and Technology Leading Project for Biosimulation and health sciences research grant (H18-Research on Human Genome-002) from the Ministry of Health, Labor, and Welfare, Japan (Dr Shimizu); (3) grant 2000.059 from the Nederlandse Hartstichting, Amsterdam, the Netherlands (Dr Wilde); and (4) research grants from the National Institutes of Health (HD42569), American Heart Association (Established Investigator Award), CJ Foundation for SIDS, and Dr Scholl Foundation (Dr Ackerman).

Disclosures

Dr Ackerman is a consultant for Clinical Data (formerly Genaissance Pharmaceuticals) with respect to the FAMILION genetic test for cardiac ion channel mutations. The other authors report no conflicts.

References

1. Moss AJ. Long QT syndrome. *JAMA*. 2003;289:2041–2044.
2. Wilde AA, Bezzina CR. Genetics of cardiac arrhythmias. *Heart*. 2005; 91:1352–1358.
3. Sanguinetti MC. Long QT syndrome: ionic basis and arrhythmia mechanism in long QT syndrome type 1. *J Cardiovasc Electrophysiol*. 2000;11:710–712.
4. Tester DJ, Will ML, Haglund CM, Ackerman MJ. Compendium of cardiac channel mutations in 541 consecutive unrelated patients referred for long QT syndrome genetic testing. *Heart Rhythm*. 2005;2:507–517.
5. Bianchi L, Priori SG, Napolitano C, Surewicz KA, Dennis AT, Memmi M, Schwartz PJ, Brown AM. Mechanisms of I(Ks) suppression in LQT1 mutants. *Am J Physiol*. 2000;279:H3003–H3011.
6. Shalaby FY, Levesque PC, Yang WP, Little WA, Conder ML, Jenkins-West T, Blanar MA. Dominant-negative KvLQT1 mutations underlie the LQT1 form of long QT syndrome. *Circulation*. 1997;96: 1733–1736.
7. Zareba W, Moss AJ, Sheu G, Kaufman ES, Priori S, Vincent GM, Towbin JA, Benhorin J, Schwartz PJ, Napolitano C, Hall WJ, Keating MT, Qi M, Robinson JL, Andrews ML. Location of mutation in the KCNQ1 and phenotypic presentation of long QT syndrome. *J Cardiovasc Electrophysiol*. 2003;14:1149–1153.
8. Shimizu W, Horie M, Ohno S, Takenaka K, Yamaguchi M, Shimizu M, Washizuka T, Aizawa Y, Nakamura K, Ohe T, Aiba T, Miyamoto Y, Yoshimasa Y, Towbin JA, Priori SG, Kamakura S. Mutation site-specific differences in arrhythmic risk and sensitivity to sympathetic stimulation in the LQT1 form of congenital long QT syndrome: multicenter study in Japan. *J Am Coll Cardiol*. 2004;44:117–125.
9. Cox DR. Regression models and life-tables. *J Stat Soc [B]*. 1972;34: 187–220.
10. Therneau TM, Grambsch PM. *Modeling Survival Data: Extending the Cox Model*. New York, NY: Springer-Verlag; 2000.
11. Sanguinetti MC, Jiang C, Curran ME, Keating MT. A mechanistic link between an inherited and an acquired cardiac arrhythmia: HERG encodes the IKr potassium channel. *Cell*. 1995;81:299–307.
12. Wang Q, Shen J, Li Z, Timothy K, Vincent GM, Priori SG, Schwartz PJ, Keating MT. Cardiac sodium channel mutations in patients with long QT

syndrome, an inherited cardiac arrhythmia. *Hum Mol Genet*. 1995;4:1603–1607.
13. Vatta M, Ackerman MJ, Ye B, Makielski JC, Ughanze EE, Taylor EW, Tester DJ, Balijepalli RC, Foell JD, Li Z, Kamp TJ, Towbin JA. Mutant caveolin-3 induces persistent late sodium current and is associated with long-QT syndrome. *Circulation*. 2006;114:2104–2112.
14. Splawski I, Shen J, Timothy KW, Lehmann MH, Priori S, Robinson JL, Moss AJ, Schwartz PJ, Towbin JA, Vincent GM, Keating MT. Spectrum of mutations in long-QT syndrome genes: KVLQT1, HERG, SCN5A, KCNE1, and KCNE2. *Circulation*. 2000;102:1178–1185.
15. Shimizu W, Noda T, Takaki H, Nagaya N, Satomi K, Kurita T, Suyama K, Aihara N, Sunagawa K, Echigo S, Miyamoto Y, Yoshimasa Y, Nakamura K, Ohe T, Towbin JA, Priori SG, Kamakura S. Diagnostic value of epinephrine test for genotyping LQT1, LQT2, and LQT3 forms of congenital long QT syndrome. *Heart Rhythm*. 2004;1:276–283.
16. Sanguinetti MC, Curran ME, Zou A, Shen J, Spector PS, Atkinson DL, Keating MT. Coassembly of K(V)LQT1 and minK (IsK) proteins to form cardiac I(Ks) potassium channel. *Nature*. 1996;384:80–83.
17. Aizawa Y, Ueda K, Wu LM, Inagaki N, Hayashi T, Takahashi M, Ohta M, Kawano S, Hirano Y, Yasunami M, Kimura A, Hiraoka M. Truncated KCNQ1 mutant, A178fs/105, forms hetero-multimer channel with wild-type causing a dominant-negative suppression due to trafficking defect. *FEBS Lett*. 2004;574:145–150.
18. Hobbs JB, Peterson DR, Moss AJ, McNitt S, Zareba W, Goldenberg I, Qi M, Robinson JL, Sauer AJ, Ackerman MJ, Benhorin J, Kaufman ES, Locati EH, Napolitano C, Priori SG, Towbin JA, Vincent GM, Zhang L. Risk of aborted cardiac arrest or sudden cardiac death during adolescence in the long-QT syndrome. *JAMA*. 2006;296:1249–1254.
19. Moss AJ, Schwartz PJ, Crampton RS, Tzivoni D, Locati EH, MacCluer J, Hall WJ, Weitkamp L, Vincent GM, Garson A Jr. The long QT syndrome: prospective longitudinal study of 328 families. *Circulation*. 1991;84:1136–1144.
20. Locati EH, Zareba W, Moss AJ, Schwartz PJ, Vincent GM, Lehmann MH, Towbin JA, Priori SG, Napolitano C, Robinson JL, Andrews M, Timothy K, Hall WJ. Age- and sex-related differences in clinical manifestations in patients with congenital long-QT syndrome: findings from the International LQTS Registry. *Circulation*. 1998;97:2237–2244.
21. Zareba W, Moss AJ, Locati EH, Lehmann MH, Peterson DR, Hall WJ, Schwartz PJ, Vincent GM, Priori SG, Benhorin J, Towbin JA, Robinson JL, Andrews ML, Napolitano C, Timothy K, Zhang L, Medina A. Modulating effects of age and gender on the clinical course of long QT syndrome by genotype. *J Am Coll Cardiol*. 2003;42:103–109.
22. Tsuji K, Akao M, Ishii TM, Ohno S, Makiyama T, Takenaka K, Doi T, Haruna Y, Yoshida H, Nakashima T, Kita T, Horie M. Mechanistic basis for the pathogenesis of long QT syndrome associated with a common splicing mutation in KCNQ1 gene. *J Mol Cell Cardiol*. 2007;42:662–669.

CLINICAL PERSPECTIVE

Type-1 long-QT syndrome is caused by loss-of-function mutations in the KCNQ1-encoded I_{Ks} cardiac potassium channel. In the present study involving 600 patients having a spectrum of KCNQ1 mutations derived from 3 long-QT syndrome registries, we found that cardiac event rates are increased significantly in patients with mutations located in the transmembrane region of the potassium channel and in patients with mutations having a putative dominant-negative effect on the repolarizing I_{Ks} current. The effects of these genetically determined factors are independent of traditional clinical risk factors and of β-blocker therapy. Mutation location and knowledge of functional effects of the mutation provide additional risk information beyond the clinical risk factors and the genotype, at least for type-1 long-QT syndrome, and this information should contribute to improved risk stratification and more focused management of these higher-risk patients.